$\delta^{11}B$ as monitor of calcification site pH in marine calcifying organisms

Jill N. Sutton[1], Yi-Wei Liu[1], Justin B. Ries[2], Maxence Guillermic[1], Emmanuel Ponzevera[3], and Robert A. Eagle [1,4,5]

[1]Université de Brest, UBO, CNRS, IRD, Ifremer, Institut Universitaire Européen de la Mer, LEMAR, Rue Dumont d'Urville, 29280, Plouzané, France
[2]Department of Marine and Environmental Sciences, Marine Science Center, Northeastern University, 430 Nahant Rd, Nahant, MA 01908, USA
[3]Unité de Recherche Géosciences Marines, Ifremer, 29280, Plouzané, France
[4]Institute of the Environment and Sustainability, University of California, Los Angeles, LaKretz Hall, 619 Charles E Young Dr E #300, Los Angeles, CA 90024, USA
[5]Atmospheric and Oceanic Sciences Department, University of California – Los Angeles, Maths Science Building, 520 Portola Plaza, Los Angeles, CA 90095, USA

Correspondence to: Jill-Naomi.Sutton@univ-brest.fr and robeagle@g.ucla.edu

Abstract. The boron isotope composition ($\delta^{11}B$) of marine biogenic carbonates has been predominantly studied as a proxy for monitoring past changes in seawater pH and carbonate chemistry. In order to derive seawater pH from skeletal boron isotope ratio data, a number of assumptions related to chemical kinetics and themodynamic isotope exchange reactions are necessary. Furthermore, the boron isotope composition of biogenic carbonates ($\delta^{11}B_{CaCO3}$) is assumed to reflect the $\delta^{11}B$ of dissolved borate ($B(OH)_4^-$) in seawater. Here we report the development of methodology for measuring the $\delta^{11}B$ in biogenic carbonate samples at the multi-collector inductively coupled mass spectrometry facility at Ifremer (Plouzané, France) and the evaluation of $\delta^{11}B_{CaCO3}$ in a diverse range of marine calcifying organisms. We evaluated the $\delta^{11}B_{CaCO3}$ of 6 species of marine calcifiers (a temperate coral, *Oculina arbuscula*; a coralline red alga, *Neogoniolithion* sp.*;* a tropical urchin, *Eucidaris tribuloides*; a temperate urchin, *Arbacia punctulata*; a serpulid worm, *Hydroides crucigera;* and an American oyster, *Crassostrea virginica*) that were reared for 60 days in isothermal seawater (25°C) equilibrated with an atmospheric pCO_2 of *ca.* 409 µatm. We observe large inter-species variability in $\delta^{11}B_{CaCO3}$ (*ca.* 20 ‰) and significant discrepancies between measured $\delta^{11}B_{CaCO3}$ and $\delta^{11}B_{CaCO3}$ expected from established relationships between $\delta^{11}B_{CaCO3}$ and seawater pH. We discuss these results in the context of various proposed mechanisms of biocalcification, including the potentially critical role that internal calcifying site pH plays in regulating $CaCO_3$ saturation state and borate $\delta^{11}B$ at the site of calcification and, thus, the $\delta^{11}B$ composition of calcifers' shells and skeletons.

1 Introduction

The ability to monitor historical changes in seawater pH on both short and long-term timescales is necessary to understand the influence that dramatic changes in atmospheric CO_2 (pCO_2) have had on marine carbonate chemistry. The recent anthropogenic increase in pCO_2 has already resulted in a significant decrease in seawater pH (Bates, 2007; Feely et al., 2008; Dore et al., 2009; Byrne et al., 2010; Gonzalez-Davlia et al., 2010; IPCC, 2014; Feely et al., 2016), with potential effects on the ability of marine calcifying organisms to produce skeletal calcium carbonate ($CaCO_3$; IPCC, 2014). Ocean acidification studies have revealed that organismal responses vary widely amongst taxa, highlighting the complexity of biological responses to ocean acidification (e.g., Ries et al., 2009; Kroeker et al., 2010; Kroeker et al., 2013) and necessitating a more complete understanding of how an organism's mechanism of biocalcification governs its specific response to ocean acidification.

1.1 Theoretical model of $\delta^{11}B$ variation with pH

The boron isotope composition ($\delta^{11}B$) of biogenic $CaCO_3$ ($\delta^{11}B_{CaCO3}$) has been primarily used as a palaeoceanographic proxy for seawater pH (Hönisch and Hemming, 2004; Hönisch et al., 2004; Montagna et al., 2007; Palmer, 1998; Pearson et al.,

2009; Penman and Hönisch, 2014; Rae et al., 2011; Trotter et al., 2011; Vengosh et al., 1991; Wei et al., 2009). Boron has a residence time in seawater of *ca.* 14 million years (Lemarchand et al., 2000), which is much longer than the mixing time of oceans (*ca.* 1000 years), suggesting that it behaves conservatively (Foster et al., 2010), making $\delta^{11}B$ an attractive palaeo-proxy for pH. The development of this proxy is based on a theoretical model of $\delta^{11}B$ variation with pH (Zeebe and Wolf-Gladrow, 2001) that assumes that $\delta^{11}B_{CaCO3}$ reflects the $\delta^{11}B$ composition of borate in seawater ($\delta^{11}B_{B(OH)4-}$; Hemming and Hanson, 1992). The theoretical model of $\delta^{11}B$ variation as a function of pH requires knowledge of the fractionation factor (α) for isotope exchange between the aqueous species of boron, the dissociation constant (pK_B), and the isotopic composition of boron in seawater (Pagani et al., 2005).

Boron exists in aqueous solutions as either trigonal boric acid [$B(OH)_3$] or as the tetrahedral borate anion [$B(OH)_4^-$] and their proportions in solution are pH dependent (Fig. 1), as defined by the following equilibrium reaction:

$$B(OH)_3 + H_2O \leftrightarrow B(OH)_4^- + H^+$$

In modern seawater, $B(OH)_4^-$ represents ~24.15 % of boron species, assuming that the dissociation constant (pK_B) between these two species of boron is 8.597 (at 25 °C, pH = 8.1; Dickson, 1990). Boron has two stable isotopes (^{10}B and ^{11}B) with relative abundances of 19.9 % and 80.1 %, respectively, and $B(OH)_3$ is enriched in ^{11}B relative to $B(OH)_4^-$ due to molecular differences of these chemical species in solution. The isotopic composition of boron is expressed following standard convention:

$$\delta^{11}B = [(^{11}B_{sample}/^{10}B_{sample})/(^{11}B_{standard}/^{10}B_{standard})\text{-}1] \times 1000\ (‰); \quad (1)$$

where the reference standard is NIST SRM 951 (Catanzaro et al, 1970).

The $\delta^{11}B$ of modern seawater is 39.61 ± 0.20 ‰ (Foster et al., 2010) and a large (> 20‰) and constant α exists between the two aqueous species described above. The α between boric acid and borate ion is defined as:

$$\alpha \equiv \frac{(11B/10\ )_{Boric\ acid}}{(11B/10B)_{Borate\ ion}};$$

A wide range of theoretical and empirical values for α have been suggested (Byrne et al., 2006; Kakihana et al., 1977; Klochko et al., 2006; Nir et al., 2015; Palmer et al., 1987). For example, α = 1.0194 was calculated from theory by Kakihana et al. (1977) and was widely applied in palaeo-reconstructions of seawater pH (Hönisch et al., 2004; Kakihana et al., 1977; Sanyal et al., 1995). Zeebe (2005) used analytical techniques and *ab initio* molecular orbital theory to calculate α ranging from 1.020 to 1.050 at 300 K. Zeebe (2005) provided several arguments in support of $\alpha \geqq 1.030$, ultimately concluding that experimental work was required to determine the α between dissolved boric acid and the borate ion. Subsequent to the work by Zeebe (2005), significant error was identified for the borate vibrational spectrum term used in Kakihana et al.'s (1977) theoretical calculation of α (Klochko et al., 2006; Rustad and Bylaska, 2007). An empirical α of 1.0272 (Klochko et al., 2006), using a corrected borate vibrational spectrum term, is now considered to best describe the boron isotope fractionation between dissolved boric acid and borate ion in seawater (Rollion-Bard and Erez, 2010; Xiao et al., 2014). Moreover, due to the ability of some calcifying organisms to alter carbonate chemistry at their site of calcification, empirical species-specific calibrations between $\delta^{11}B_{CaCO3}$ and seawater pH (pH_{SW}) are likely more appropriate than theoretical α values if the goal is to reconstruct ambient seawater conditions (Anagnostou et al., 2012; Hönisch et al., 2004; Krief et al., 2010; Rae et al., 2011; Reynaud et al., 2004; Trotter et al., 2011).

The most widely applied framework in which the boron isotope composition of carbonates is interpreted relies on the assumption that $B(OH)_4^-$ is the dominant species of dissolved inorganic boron incorporated into $CaCO_3$ minerals as they precipitate from solution. It is also well established that $\delta^{11}B$ of $B(OH)_4^-$ is controlled by solution pH (c.f. Hemming and Hönisch, 2007; see discussion above). Therefore, $\delta^{11}B_{CaCO3}$ should reflect pH of the precipitating solution, which is consistent with the observations of a number of empirical studies (see Hemming and Hönisch, 2007, for summary). More recently alternative models of boron incorporation into $CaCO_3$ have been proposed (Klochko et al., 2009; Noireaux et al., 2015; Uchikawa et al., 2015; Balan et al., 2016). Generally speaking, these alternative models present a potential challenge to the utility of boron isotopes to reconstruct calcifying fluid and paleo-pH (Klochko et al., 2009 ; Noireaux et al., 2015; Uchikawa et al., 2015; Mavromatis et al., 2015; Balan et al., 2016). They present evidence consistent with boric acid, alongside borate, incorporation into some carbonates (eg. Noireaux et al., 2015; Uchikawa et al., 2015) and/or the presence trigonal boron in the carbonate lattice due to transformation from borate during precipitation (e.g. Mavromatis et al., 2015). Some of these studies also highlight that calcite may be more prone to this complication than aragonite (e.g. Noireaux et al., 2015). Here, as an alternative hypothesis to a primary pH control over biomineral $\delta^{11}B$ composition, we also consider the compatibility of our data with the different models of boron incorporation.

1.2 The role of calcification site pH in calcareous biomineralization and organisms' responses to ocean acidification

Many calcifying marine organisms, including scleractinian corals (Al-Horani et al., 2003; Cohen and Holcomb, 2009; Cohen and McConnaughey, 2003; Holcomb et al., 2010; Ries, 2011a), coralline red algae (Borowitzka and Larkum, 1987; McConnaughey and Whelan, 1997), calcareous green algae (De Beer and Larkum, 2001; Borowitzka and Larkum, 1987; McConnaughey and Falk, 1991), foraminifera (Rink et al., 1998; Zeebe and Sanyal, 2002), and crabs (Cameron, 1985) are thought to facilitate precipitation of their skeletal or shell $CaCO_3$ by elevating pH at their site of calcification. The effect of pH on $CaCO_3$ chemistry at the site of calcification can be summarized by the following equilibrium reactions:

$$H_2CO_3 \leftrightarrow HCO_3^- + H^+$$

and

$$HCO_3^- \leftrightarrow H^+ + CO_3^{2-};$$

which are respectively governed by the following stoichiometric dissociation constants:

$$K^*_1 = [HCO_3^-][H^+]/[H_2CO_3]$$

and

$$K^*_2 = [CO_3^{2-}][H^+]/[HCO_3^-]$$

Thus, reducing $[H^+]$ at the site of calcification shifts the carbonic acid system towards elevated $[CO_3^{2-}]$, thereby increasing $CaCO_3$ saturation state (Ω_{CaCO3}) following:

$$\Omega_{CaCO3} = [Ca^{2+}][CO_3^{2-}]/K^*_{sp}$$

where K^*_{sp} is the stoichiometric solubility product of the appropriate $CaCO_3$ polymorph (e.g., calcite, aragonite, etc.) and is influenced by temperature and salinity.

The decrease in pH_{SW} that will accompany the forecasted rise in anthropogenic atmospheric pCO_2 will reduce seawater $[CO_3^{2-}]$, which has been shown to inhibit biological deposition of $CaCO_3$, or even promote its dissolution (c.f. Doney et al., 2009; Fabry et al., 2008; Kleypas et al., 2006; Kroeker et al. 2010; Langdon, 2002; Ries et al., 2009). However, if seawater is the

source of an organism's calcifying fluid (e.g., Gaetani and Cohen, 2006), then the concentration of dissolved inorganic carbon (DIC) in this fluid will increase as atmospheric pCO_2 increases. Organisms able to strongly regulate pH of their calcifying fluid (pH_{CF}), despite reduced external pH, should convert much of this increased DIC, occurring primarily as HCO_3^-, back into the CO_3^{2-} that they need for calcification (Ries, 2011a, 2011b; Ries et al., 2009). Thus, an organism's specific response to CO_2-induced ocean acidification is critically dependent upon that organisms' ability to regulate pH at their site of calcification.

It should be noted that marine calcifiers biomineralize in diverse ways, and that some calcifers' mechanisms of biomineralization are better understood than others. Corals are thought to accrete $CaCO_3$ directly from a discrete calcifying fluid (e.g., Cohen and McConnaughey, 2003 and references therein; Al-Horani et al., 2003; Cohen and Holcomb, 2009; Gaetani and Cohen, 2006; Ries, 2011a), with mineralization sites and crystal orientations being influenced by organic templates and/or calicoblastic cells (e.g., Cuif and Dauphin, 2005; Goldberg, 2001; Meibom et al., 2008; Tambutté et al., 2007). Mollusks are also thought to precipitate their shells from a discrete calcifying fluid between the external epithelium of the mantle and the inner layer of the shell known as the extrapallial fluid (e.g., Crenshaw, 1972), with hemocytes and organic templates playing a potentially important role in crystal nucleation (e.g., Mairie et al., 2012; Mount et al., 2004; Weiner et al., 1984). Coralline red algae, such as those belonging to the family Corallinaceae, are also thought to precipitate high-Mg calcite (and/or aragonite) crystals from an intercellular calcifying fluid (Simkiss and Wilbur, 1989). Notably, biomineralization by coralline red algae occurs primarily within the cell wall and often has a preferred crystal orientation, which is not typical of other calcifying macroalgae (Simkiss and Wilbur, 1989). Echinoids, in contrast, are thought to initiate calcification on Ca^{2+}-binding organic matrices within cellular vacuoles (Ameye et al., 1998).

Various mechanisms have been proposed for elevating pH_{CF}, including conventional H^+-channeling (McConnaughey and Falk, 1991), Ca^{2+}-H^+ exchanging ATPase (Cohen and McConnaughey, 2003; McConnaughey and Falk, 1991; McConnaughey and Whelan, 1997), light-induced H^+-pumping (De Beer and Larkum, 2001), transcellular symporter and co-transporter H^+- solute shuttling (McConnaughey and Whelan, 1997), cellular extrusion of hydroxyl ions (OH^-) into the calcifying medium, and CO_2-consumption via photosynthesis (e.g., Borowitzka and Larkum, 1976).

Regardless of the exact composition (e.g., seawater vs. modified seawater) or nature (e.g., fluid vs. gel) of their calcifying media, or the specific mechanisms by which they produce their $CaCO_3$ (e.g., organic templates vs. cellular mediation vs. proton-pumps vs. Ca^{2+}-ATPase), an organism's ability to control pH_{CF} should strongly influence their ability to convert DIC into CO_3^{2-}, thereby impacting their specific calcification response to CO_2-induced ocean acidification.

1.3 Relationship between calcification site pH and $\delta^{11}B_{CaCO3}$

Organisms that precipitate $CaCO_3$ from a discrete calcifying fluid may record in their shells and skeletons $\delta^{11}B_{CaCO3}$ compositions that reflect pH_{CF} of their calcifying fluid (McCulloch et al., 2012 Holcomb et al., 2014; Farmer et al., 2015; Martin et al., 2016). Numerous studies have documented a relationship between the pH_{SW} and the $\delta^{11}B_{CaCO3}$ composition of foraminiferal shells and coral skeletons (Fig. 2). However, the observed relationships between biogenic $\delta^{11}B_{CaCO3}$ and pH_{SW} vary widely amongst taxa (Fig. 2), and generally differ from that measured or derived theoretically for $B(OH)_4^-$ in seawater (Byrne et al., 2006; Klochko et al., 2006; Liu and Tossell, 2005; Zeebe, 2005) and from that observed in abiotically precipitated $CaCO_3$ (Sanyal et al., 2000; Noireaux et al., 2015).

One hypothesis for the discrepancies between the expected $\delta^{11}B_{CaCO3}$-pH relationship and that actually observed for biogenically precipitated $CaCO_3$ is that most marine calcifiers are not precipitating their $CaCO_3$ directly from seawater, but rather from a discrete calcifying fluid with a pH_{CF} that is substantially elevated relative to that of their external seawater. Prior studies have shown that, for a given pH_{SW}, $\delta^{11}B_{CaCO3}$ of the coral species *Porites cylindrica* and *Acropora nobilis* is moderately

elevated relative to $\delta^{11}B_{CaCO3}$ of the foraminifera *Globigerinoides sacculifer* and substantially elevated relative to the mollusk *Mytilus edulis* (Fig. 2; Heinemann et al., 2012; Hönisch et al., 2004; Sanyal et al., 2001). One possible explanation for these differences is that corals are maintaining their calcifying fluids at higher pH than the calcifying fluids of foraminifera, which are in turn elevated relative to the pH_{CF} of mussels. This is consistent with pH microelectrode (Al-Horani et al., 2003; Ries, 2011a), boron isotope (e.g., Rollion-Bard et al., 2003, Rollion-Bard et al., 2011b; Anagnostou et al., 2012; Krief et al., 2010; Trotter et al., 2011; McCulloch et al., 2012; Wall et al., 2016), and fluorescent pH dye data (Venn et al., 2009, 2011, 2013), suggesting that scleractinian corals elevate their pH_{CF} to 8.5 – 10, versus their external pH_{SW} of 8, that foraminifera maintain their pH_{CF} between 8 and 9 (Jorgensen et al., 1985; Rink et al., 1998), and that bivalves maintain their pH_{CF} between 7.5 and 8 (Crenshaw, 1972).

Here, we investigate differences in $\delta^{11}B_{CaCO3}$-pH relationships amongst taxonomically diverse biogenic calcification systems and discuss the compatibility of these observations with the hypothesis that $\delta^{11}B_{CaCO3}$ of biogenic carbonate is recording pH_{CF}, rather than pH_{SW}—a key parameter of biological calcification that has proven challenging to measure yet is fundamental to understanding, and even predicting, marine calcifiers' responses to CO_2-induced ocean. By systematically investigating the $\delta^{11}B_{CaCO3}$ composition of a taxonomically broad range of taxa, each employing different mechanisms of calcification, yet all cultured under equivalent laboratory conditions (Ries et al., 2009), we are able to empirically assess biological controls on the $\delta^{11}B_{CaCO3}$ composition of biogenic carbonates.

2 Methods and materials

2.1 Laboratory conditions

Sample processing and chemical separation were performed under ISO 5 (class 100) laminar flow hoods within an ISO 6 (class 1,000) clean room at Ifremer (Plouzané, France). Analyses of $^{11}B/^{10}B$ ratios were carried out using a Thermo Scientific Neptune MC-ICP-MS at the Pôle Spectrometrie Océan (PSO), Ifremer (Plouzané, France). Efforts were made to minimize sample exposure to laboratory air.

2.2 Reagents

Ultra-pure reagents were used for all chemical procedures. The source of high-purity water (UHQ) for the procedure is a Millipore Direct-Q water purification system with a specific resistivity of 18.2 MΩ·cm. All HNO_3 solutions are obtained from dilutions using Aristar Ultra-high purity acid. The 0.5 N NH_4OH solutions are boron-cleaned by exchange with boron-specific resin (Amberlite IRA 743). UHQ water is buffered to pH 7 with the boron-cleaned NH_4OH. The reagent boron blanks were measured on a Thermo Scientific Element XR at the PSO, Ifremer (Plouzané, France) and were all < 0.1 ppb, yielding a total B blank of <100 ng per sample.

2.3 Materials

2.3.1 Samples

In this study, we evaluated the $\delta^{11}B_{CaCO3}$ of 6 highly divergent species of marine calcifiers that had been reared for 60 days in isothermal (25°C) and isosaline (32 practical salinity units; psu) seawater equilibrated with atmospheric pCO_2 of ca. 409 µatm, including a temperate coral (*Oculina arbuscula*), a coralline red alga (*Neogoniolithion sp.*), a tropical urchin (*Eucidaris tribuloides*), a temperate urchin (*Arbacia punctulata*), a serpulid worm (*Hydroides crucigera*), and an American oyster (*Crassostrea virginica*; see Ries et al., 2009 for details). The specimens were subsampled for new growth relative to a barium marker emplaced at the start of the experiment (details in Ries, 2011), homogenized, and multiple specimens per species were evaluated (Table 3).

2.3.2 Standards

A range of standards were used in this study, including: (1) the reference standard NIST SRM 951 (Catanzaro et al, 1970) for B isotope ratio and B concentration; (2) a mixture of NIST SRM 951 and a series of ICPMS SRM for B:Ca ratio (30-200 μg/mg); (3) the international coral standard (*Porites* sp.) JCp-1 (Geological Survey of Japan, Tsukuba, Japan); (4) the international giant clam standard (*Tridacna gigas*) JCt-1 (Geological Survey of Japan, Tsukuba, Japan); and (5) a laboratory coral standard (NEP; *Porites* sp.) from University of Western Australia/Australian National University (McCulloch et al., 2014).

2.4 Boron extraction procedure

Prior to boron isotope analysis, B was separated from the sample matrix using a B-specific anionic exchange resin (Amberlite IRA-743; Kiss, 1988). Amberlite IRA 743 behaves as an anion exchanger with a high affinity for B absorption at neutral to alkaline pH (i.e., will absorb B), and a low affinity for boron at acidic pH (i.e., will release B). The resin was crushed and sieved to a desired 100 – 200 mesh, then cleaned and conditioned to a pH of 7 (6.8 – 7.2).

Here, we present two methods of B extraction (batch and column chemistry), where the influence of matrix chemistry is removed through minor adjustments to the chemistry of existing B extraction techniques. These two methods were applied to various biogenic $CaCO_3$ samples (*Porites* coral, temperate urchin, giant clam, American oyster).

2.4.1 Oxidative cleaning

Samples and reference materials JCp-1, JCt-1, and NEP were cleaned with an oxidative cleaning method following the method of Barker et al. (2003). For a 2 mg sample, 200 μL of the alkaline-buffered (0.1 M NH_4OH) H_2O_2 was added to remove organic matter. Samples were placed in an ultrasonicator for 20 minutes at 50 °C to expedite cleaning. Following peroxide cleaning, samples were then submitted to multiple washes (typically 3) of UHQ water (pH = 7, 400 μL) until the pH of the supernatant matched that of the UHQ water to ensure removal of all oxidizing agent. The water was then removed from samples after centrifugation and a weak-acid leach was implemented by adding 20 μL of 0.001 M HNO_3 to each sample. Samples were then ultrasonicated for 10 minutes, centrifuged, and then the acid was removed. The samples were washed twice with pH-buffered UHQ water, centrifuged, and the water was removed. Dissolution of each sample was then performed by addition of 20 μL of 3 M HNO_3 followed by 300 μL of 0.05 M HNO_3. The pH of each sample was then adjusted to pH 7 with 0.2 M NH_4OH, following partition coefficients for the B-specific resin reported by Lemarchand et al. (2002). For both the batch and the column chemistry methods, the resin is pre-cleaned and conditioned to pH 7 prior to sample loading.

2.4.2 Column chemistry method

A column chemistry protocol for B extraction (described in table 1) was developed based on methods described by Wang et al. (2010) and Foster et al. (2013). Briefly, the columns were washed with pH-buffered MQ-H_2O (pH=7), 0.5 M HNO_3, and again with pH-buffered MQ-H_2O. The eluent was measured to ensure that it was at pH 7 prior to loading of the sample. The sample was then loaded onto the resin and washed multiple times (1500 μL x 3) with pH-buffered UHQ in order to remove any cations, and then the B was eluted in 1000 μL of 0.5 M HNO_3. Column yields were greater than 95 % (Fig. 3) and elution tails of every sample were checked with an extra 500 μL acid rinse. In all cases, this tail represented less than 1 % of B loaded. Small aliquots of each sample were measured by single collector HR-ICPMS prior to analyses by MC-ICPMS to verify the retention of B on the column and removal of other elements (e.g. Ca, Na, Ba, U).

2.4.3 Batch method

The batch method approach to B separation was conducted under closed conditions in an attempt to reduce airborne B contamination. Cleaned samples (pH 7) were transferred into acid-cleaned microcentrifuge tubes (500 µL; polypropylene) containing 5 mg of resin (see Section 2.4), which is B-cleaned in individual tubes with 500 µL of 0.5 M HNO_3, and then rinsed with 500 µL of MQ water (buffered to pH 7 with 2 % NH_4OH) three times to elute the other cations in the matrix and achieve pH 7. Tubes were then capped and shaken for 15 minutes to promote exchange of anions from the aqueous sample to the resin. Afterwards, the mixture was centrifuged (1 min, 2000 rpm), the matrix was decanted, and the resin was washed three times (200 µL) with pH-buffered (pH 7) UHQ water to elute any cations. Boron recovery was then performed with the addition of 500 µL 0.05 M HNO_3 and shaken again for 15 min to promote the anion exchange between the resin and solution. A final tail-check was performed with 100 µL of 0.05 M HNO_3 to ensure that all of the B was recovered in the initial 500 µL 0.05 M HNO_3 solution.

2.5 Procedural blanks

The total yield of B from procedural blanks, which encompasses reagent, air-borne and procedural contamination, was sub-nanogram (lowest yields for column = 0.5 ng and batch = 90 pg). Such low contamination was achieved through stringent cleaning and handling protocols for all consumables and reagents, thereby permitting accurate measurement of B at sub-µM concentrations.

2.6 Boron recovery and matrix removal

A major challenge in the measurement of $\delta^{11}B$ by MC-ICPMS is the elimination of residual boron from prior analyses (i.e., 'memory effects'). In order to evaluate memory effects, multiple concentrations (30 ppb to 130 ppb) of a standard solution (NIST SRM 951) were analysed. After washing out the MC-ICPMS with a solution of 0.05 M HNO_3 for several minutes, the residual ^{11}B and ^{10}B signals were in the range of 10 – 80 mV, equivalent to 5 % (30 ppb) and 3 % (130 ppb), respectively (see Fig. S1 for ^{11}B blanks). Boron recovery was measured using a Thermo Scientific Element XR HR-ICP-MS at the Laboratory for Geochemistry and Metallogeny, Ifremer (Plouzané, France). Boron yields are evaluated by tracking B throughout the entire procedure.

2.7 Mass spectrometry

Isotopic measurements were conducted using a Thermo Scientific Neptune MC-ICPMS at the PSO, Ifremer (Plouzané, France), operated with standard plasma settings. To account for drift in mass discrimination through the analysis, samples were bracketed by matrix-matched standards of similar composition. Typically, the concentration of the standard (NIST SRM 951) was 50 ppb in 0.05 M HNO_3. Each analysis consisted of a 2-minute simultaneous collection of masses 11 and 10 on Faraday cups H3 and L3 equipped with 10^{11} Ω resistors. Each sample was analysed in duplicate during a single analytical session, with replicate analyses not sharing a bracketing standard. As such, the boron isotope ratios are determined as delta values ($\delta^{11}B$). The $\delta^{11}B$ of the calcium carbonate standards JCp-1 (*Porites* sp.), NEP (*Porites* sp.) and JCt-1 (hard clam) standards, which were processed in the same manner and are reported in the results section (see Section 3.1.1) alongside their published reference values (Foster et al., 2013; McCulloch et al., 2014).

The MC-ICPMS method is a commonly used approach to measure $\delta^{11}B$ due to its capacity for rapid, accurate and reproducible analyses (see McCulloch et al., 2014, for a recent summary of these methods). Challenges with this method arise from the volatile and persistent nature of boron that can result in significant memory effects, cross-contamination between samples and standards, and unanticipated matrix effects (McCulloch et al. 2014; Foster et al. 2013). Given the sensitivity of $\delta^{11}B_{CaCO3}$-

based estimates of pH_{CF} to the analytical uncertainty cited above, two different injection methods (described below) were evaluated to determine what method is most suitable for minimizing analytical error.

2.7.1 Demountable direct injection nebulizer

Memory effects were addressed by introducing samples to the plasma with demountable direct injection high-efficiency nebulizer (d-DIHEN; Louvat et al., 2014). Baseline B-concentrations between samples were measured with counting times of 30 s (Table 2).

2.7.2 Ammonia addition

For the ammonia addition method, a dual inlet PFA Teflon spray chamber was used with an ESI PFA 50 µL/min nebuliser to add ammonia gas at a rate of ~3 mL/min (Al-Ammar et al., 2000; Foster, 2008). The addition of ammonia gas to the spray chamber ensures that the analyte remains alkaline, which prevents volatile boron from recondensing in the chamber during analysis (Al-Ammar et al., 2000). The measured B isotope signal of the rinse blank was then subtracted from the B isotope ratios in order to monitor B wash out, as suggested by Foster (2008). In all cases, wash out time was 200 seconds and samples were matrix- and intensity-matched to the bracketing standards.

3 Results

3.1 Method development

The yields for boron extraction for both methods were evaluated for various biogenic $CaCO_3$ samples and were typically between 97 and 102 % (determined by HR-ICPMS; see section 2.6). Washes with pH-buffered MQ-H_2O effectively removed Ca (99.9 %), Na (100 %), Ba (> 80 %), and U (> 93 %) from the sample matrix. The robustness of the methods is demonstrated by the observed agreement (represented as 2 standard deviations around the mean; 2SD) between measured values of the international $CaCO_3$ standards JCp-1 and JCt-1, a coral (*Porites* sp.; $\delta^{11}B_{NH3} = 24.45 \pm 0.28$ ‰, $\delta^{11}B_{d\text{-}DIHEN} = 24.30 \pm 0.16$ ‰) and a giant clam (*Tridacna gigas*; $\delta^{11}B = 16.65_{NH3} \pm 0.39$ ‰, $\delta^{11}B_{d\text{-}DIHEN} = 17.5 \pm 0.60$ ‰), and their values established via inter-laboratory calibration ($\delta^{11}B = 24.36 \pm 0.51$ ‰, n = 10 and 16.34 +/- 0.64 ‰, respectively; Gutjahr et al. 2014; see Table 3). In addition, both column and batch methods were evaluated using the NEP laboratory standard (*Porites* sp.), a temperate urchin, a hard clam, and an oyster. As shown in Table 3, good agreement was achieved between $\delta^{11}B_{CaCO3}$ obtained via the batch and column chemistry methods for each of the biogenic $CaCO_3$ samples analysed.

3.2 Boron isotope composition of marine biogenic $CaCO_3$

Average $\delta^{11}B_{CaCO3}$ composition for all species evaluated in this study range from 16.27 ‰ to 35.09 ‰ (Table 3). The individual and average data are presented in Tables 3 and 4, respectively, and summarized in the text that follows. Note that the variance of the data presented in Table 4 represents inter-specimen variability (i.e., variability amongst different specimens of the same species), which is substantially greater than the intra-specimen variability (i.e., variability within a specimen) and analytical variability (variability amongst repeat analyses of the same subsample of a specimen) (Table 3). The coralline red alga *Neogoniolithion sp.* (35.89 ± 3.71 ‰; n = 3) exhibited the highest $\delta^{11}B_{CaCO3}$, followed by the temperate coral *O. arbuscula* (24.12 ± 0.19 ‰; n = 3), the tube of the serpulid worm *H. crucigera* (19.26 ± 0.16 ‰; n = 3), the tropical urchin *E. tribuloides* (18.71 ± 0.26 ‰; n = 3), the temperate urchin *A. punctulata* (16.28 ± 0.86 ‰; n = 3), and the American oyster *C. virginica* (16.03 ‰; n = 1). Therefore, a range of *ca.* 20 ‰ in $\delta^{11}B_{CaCO3}$ was observed across all species evaluated in this study (Table 3 and 4). Notably, these are the first published $\delta^{11}B_{CaCO3}$ data for serpulid worm tubes and oysters.

3.3 Compatibility of the interspecific range of $\delta^{11}B_{CaCO3}$ with established seawater borate $\delta^{11}B$-pH relationships

Because the investigated species were cultured under relatively equivalent conditions (pCO_2 of 409 ± 6 µatm, 32 ± 0.2 psu, 25 ± 0.1 °C; see Ries et al. 2009), differences in pH_{SW} could not have been a significant driver of the observed interspecific variability in $\delta^{11}B_{CaCO3}$ (*ca.* 20 ‰; Tables 3 and 4). In order to evaluate this *ca.* 20 ‰ interspecific variability in $\delta^{11}B$, the data are plotted against measured pH_{SW} and graphically compared with theoretical borate $\delta^{11}B$-pH curves often used to interpret $\delta^{11}B_{CaCO3}$ data in the context of pH_{SW} (Fig. 4). Clear offsets from the seawater borate $\delta^{11}B$-pH curve (Klochko et al., 2006) can be observed for several of the species: the temperate coral (*O. arbuscula*) and coralline red alga (*Neogoniolithion* sp.) fall above the curve, the temperate urchin (*A. punctulata*) and American oyster (*C. virginica*) fall below the curve, and the tube of the serpulid worm (*H. crucigera*) and the tropical urchin (*E. tribuloides*) fall nearly on the curve (see Fig. 4 and Table 3). The interpretation of these offsets from the seawater borate $\delta^{11}B$-pH curve is discussed below.

4 Discussion

4.1 Appropriateness of method for analysing $\delta^{11}B_{CaCO3}$ in marine $CaCO_3$ samples

This study describes extensive method development and analytical validation used to establish stable boron isotope measurements at Ifremer (Plouzané, France), including comparisons of different techniques for sample preparation and sample introduction to the mass spectrometer. For each of the samples evaluated, neither cleaning protocol, nor method of sample preparation, nor injection system was found to cause a significant difference in $\delta^{11}B_{CaCO3}$ composition of the samples (Table 3). The most effective method for minimizing memory effects in the MC-ICPMS analyses was found to be d-DIHEN (Louvat *et al.*, 2011). However, d-DIHEN has a complicated set-up and often generates capillary blockages arising from the aspiration of particles (e.g., resin), and/or from plasma extinction resulting from air bubble introduction. In short, sample analysis via d-DIHEN requires nearly continuous use to maintain its stability. In contrast, the ammonia-addition method (Al-Ammar *et al.*, 1999, 2000) requires continuous attention by personnel while in use, due to the use of ammonia gas, but is set-up and disassembled with relative ease between uses. We found that a constant ammonia flow of 3 mL/min was necessary to maintain a sufficiently high pH to enable a fast rinse. Less than a 3 % boron memory effect was stable after 2 minutes, enabling a signal correction for the sample that follows. Both the column and batch method of B separation yielded low blanks when < 60 µL of resin was used (see sections 2.5 and 2.6). However, the batch method was identified as preferable over the column chemistry method since the batch method has a reduced risk of B contamination due to reduced contact time with air and the small volumes of both resin and acids used in the separation process.

4.2 The $\delta^{11}B_{CaCO3}$ compositions of a diverse range of marine calcifiers

The six species investigated exhibited a broad spectrum of $\delta^{11}B_{CaCO3}$ compositions, ranging from 16.03 ‰ to 35.89 ‰ (Table 4). Assuming that only the borate ion is incorporated into $CaCO_3$ structures, the wide variation in $\delta^{11}B_{CaCO3}$ (*ca.* 20 ‰) amongst the investigated species, reared under equivalent thermo-chemical conditions, may arise from inherent differences in pH_{CF} amongst the species. If this is the case, then the observed range in $\delta^{11}B_{CaCO3}$ amongst the species (16.03 ‰ to 35.89 ‰) translates to an approximate range in pH_{CF} of 7.9 – 9.4.

Boron co-precipitation with inorganic (i.e., abiogenic) $CaCO_3$ is known to be dependent on solution pH and inorganic $CaCO_3$ precipitation rate. However, the relative abundances of the inorganic B species in solution that are incorporated into inorganic $CaCO_3$ (borate ion and boric acid) have been shown to be independent of parent solution pH (Mavromatis et al. 2015). Although Mavromatis et al. (2015) also found that polymorph mineralogy influences both the B/Ca ratio (higher in aragonite than calcite) and speciation of B in inorganic $CaCO_3$ (borate/boric acid ratio higher in aragonite than in calcite), B incorporation alone does not appear to influence boron isotope fractionation (Noireaux et al. 2015). Furthermore, because the borate/boric

acid ratio is higher in aragonite than in calcite, aragonite-producing species (corals, serpulid worms) should have a universally lower $\delta^{11}B_{CaCO3}$ composition than calcite-producing species (urchins, coralline algae, oysters) if shell mineralogy was the primary driver of the observed interspecific variation in $\delta^{11}B_{CaCO3}$ compositions – a trend that is not observed (Fig. 4). Thus, interspecific differences in polymorph mineralogy cannot, alone, explain the species' disparate $\delta^{11}B_{CaCO3}$ compositions. The more parsimonious explanation for these observed differences in $\delta^{11}B_{CaCO3}$ appears to be differences pH_{CF}, which would change the speciation of dissolved B at the site of calcification, and therefore the isotopic composition of the borate ion that is preferentially incorporated into the organisms' $CaCO_3$.

Significant deviations from equilibrium exist in the stable isotopic compositions (e.g., O, C, B) of biogenic marine $CaCO_3$ (e.g., Hemming and Hanson, 1992; McConnaughey, 1989). Notably, many marine calcifiers have $\delta^{11}B$ values that differ from the $\delta^{11}B$ composition of borate ions dissolved in seawater at an equivalent pH (Figs. 3 and 5). When interpreted in the context of the framework that skeletal $\delta^{11}B$ reflects pH_{CF} rather than pH_{SW} of the organism's surrounding seawater, these results suggest that marine calcifiers are precipitating their $CaCO_2$ from a discrete fluid with a pH_{CF} higher than, equal to, or, for some species, below that of seawater. A second hypothesis is that whilst seawater pH exerts some control over borate $\delta^{11}B$ at the site of calcification and, hence, $\delta^{11}B_{CaCO3}$, there are other species-specific effects that may influence $\delta^{11}B_{CaCO3}$ composition. The compatibility of these two hypotheses with existing models of biomineralization and observed $\delta^{11}B_{CaCO3}$ for the various marine calcifiers investigated in the present study are discussed below.

4.2.1 Temperate coral

The average $\delta^{11}B_{CaCO3}$ for the temperate coral *O. arbuscula* evaluated in this study (24.12 ± 0.19 ‰; n = 3; Tables 3 and 4) is consistent with previously published values for aragonitic corals (Table 5; see references therein). Generally, aragonitic corals are enriched in ^{11}B when compared with a theoretical borate $\delta^{11}B$-pH curve (see Figures 2 and 4). The main vital effect typically used to describe ^{11}B-enrichment in corals, relative to seawater, is an increase in pH_{CF} at the coral's site of calcification (e.g., Rollion-Bard et al., 2011b; Trotter et al., 2011; Anagnostou et al., 2012; McCulloch et al., 2012; Wall et al., 2016). This hypothesis is supported by *in situ* measurements of pH using microelectrodes (e.g., Al-Horani et al., 2003; Ries, 2011) and pH-sensitive fluorescent dyes (Venn et al., 2009, 2011, 2013).

4.2.2 Coralline red alga

The average $\delta^{11}B_{CaCO3}$ for the branching, nonarticulated coralline red alga *Neogoniolithion* sp. evaluated in this study (35.89 ± 3.71 ‰; n = 3; Tables 3 and 4) is higher than the $\delta^{11}B_{CaCO3}$ composition of any other calcifying marine organism evaluated to date (Table 5). Of particular interest, one of the coralline red alga specimens evaluated in this study exhibited $\delta^{11}B_{CaCO3}$ (39.94 ‰, Table 3) similar to the average $\delta^{11}B_{SW}$ (i.e., comprising the $\delta^{11}B$ composition of both dissolved borate and boric acid; 39.61 ‰) determined by Foster et al. (2010), raising the possibility that coralline red alga incorporate both species of dissolved inorganic boron during calcification. In support of this argument, Cusack et al. (2015) provide NMR data indicating that 30 % of the B incorporated into the coralline red alga *Lithothamnion glaciale* was present as boric acid. However, since the coralline red algae were reared at a pH_{SW} of 8.1, the $\delta^{11}B_{CaCO3}$ compositions observed for the coralline algae in the present study would require incorporation of both inorganic species of boron at $[B(OH)_3]$:$[B(OH)_4^-]$ ratios of ca. 75:25, which is not consistent with prior observations for inorganic and organic calcite (e.g., Cusack et al., 2015, reported30% trigonal boron in the calcite lattice of a different species of coralline algae).Therefore, boric acid incorporation cannot alone rule out pH_{CF} as a potential driver of the anomalously elevated $\delta^{11}B_{CaCO3}$ observed here for coralline algae.). Moreover, although nuclear magnetic resonance spectroscopy reveals that trigonal boron is present in the calcite lattice, it cannot determine whether boric acid was incorporated directly into the calcite lattice, or if the trigonal boron originated from borate post-mineralization (e.g.,

see alternative mechanisms of boron incorporation discussed in Klochko, 2006; Noireaux et al., 2015). Nevertheless, if 30% ofskeletal B is indeed directly incorporated into the calcite lattice of coralline algal skeleton, as reported by Cusack et al. (2015), pH_{CF} would still need to be as high as 9 to explain the anomalously high $\delta^{11}B_{CaCO3}$ (see Fig. 5). Short et al. (2015) observed that epiphytic turf algae can increase pH_{SW} up to 9 within the diffusive boundary layer above coralline algal crusts, driven by the algae's photosynthetic drawdown of aqueous CO_2, lending support to the idea that coralline red algae could maintain their calcifying fluid near pH 9. Thus, $\delta^{11}B_{CaCO3}$ compositions of coralline red algae may indeed reflect substantiallyelevated pH_{CF} (9.4; Table 4, Fig. 4), suggesting that coralline red algae are highly efficient at removing protons and/or dissolved inorganic carbon from their calcifying medium.

4.2.3 Tropical and temperate urchins

The average $\delta^{11}B_{CaCO3}$ for the tropical urchin *E. tribuloids* (18.71 ± 0.26 ‰; n = 3; Tables 3 and 4) and the temperate urchin *A. punctulata* (16.28 ± 0.86 ‰; n = 3; Tables 3 and 4), both evaluated in this study and reared at equivalent seawater conditions (pH_{SW} = 8.0; 25 °C; 32 psu; Table 4), are less than $\delta^{11}B_{CaCO3}$ previously reported for other echinoid species (see Table 4; 22.7 ‰ - 22.8 ‰) but are close to theoretical values of dissolved borate at those seawater conditions (17.33 ‰; Fig. 4). Microelectrode evidence suggests that urchins calcify from fluids with a pH_{CF} and composition similar to that of seawater (Stumpp et al. 2012), which is supported by our observation that urchin $\delta^{11}B_{CaCO3}$ is similar to $\delta^{11}B$ of dissolved borate. The difference between the $\delta^{11}B_{CaCO3}$ of these two species of urchin and the theoretical value of $\delta^{11}B$ for seawater borate (17.33 ‰) is +1.38 ‰ for the tropical urchin and -1.05 ‰ for the temperate urchin – a difference that exceeds their interspecimen variability (± 0.26 ‰ for the tropical urchin; ± 0.86 ‰ for the temperate urchin, determined as standard deviation (SD), see Table 5). However, the urchins could achieve this deviation in $\delta^{11}B_{CaCO3}$ by adjusting pH of their calcifying environment by only ± 0.1 units (e.g., pH_{CF} of 8.1 and 7.9 yield $\delta^{11}B$ of calcification site borate of 18.38‰ and 16.42 ‰, respectively; see table 4). Thus, if deviations in urchin $\delta^{11}B_{CaCO3}$ from seawater borate $\delta^{11}B$ indeed reflect urchins' ability to modify pH at their site of calcification, these modifications appear to be relatively minor (i.e., ± 0.1 pH units) and not always in a direction that favours calcification—consistent with Stumpp et al.'s (2012) observation that urchin biomineralization can occur in cellular compartments where pH_{CF} is lower than that of seawater. Note that the $\delta^{11}B$ values for these high-Mg calcite-precipitating organisms are also not consistent with significant boric acid incorporation into the carbonate lattice (Fig. 5).

4.2.4 Serpulid worm tube

The average $\delta^{11}B_{CaCO3}$ for the calcareous tube of the serpulid worm *H. crucigera* evaluated in this study (19.26 ± 0.16 ‰; n = 3; Tables 3 and 4) is close to theoretical value of $\delta^{11}B$ for seawater borate (Fig. 4). The serpulid worm *H. crucigera* secretes their calcareous tube from a combination of aragonite and high-Mg calcite (HMC; Ries, 2011b). The worms initiallyproduce a slurry of $CaCO_3$ granules in a pair of anterior glands, which ultimately coalesces within a matrix of inorganic and organic components (Hedley, 1956). The samples of *H. crucigera* evaluated in this study were exposed to environmental conditions (pH_{SW} = 8.1; 25 °C; 32 psu; Table 4) yielding a theoretical seawater borate $\delta^{11}B$ and, thus, $\delta^{11}B_{CaCO3}$ of 18.38 ‰, which is 0.88 ‰ less than $\delta^{11}B_{CaCO3}$ measured for *H. crucigera.* Similar to the tropical urchin discussed above, the serpulid worm could generate this divergence in $\delta^{11}B_{CaCO3}$ from seawater borate $\delta^{11}B$ by elevating pH_{CF} by 0.08 units relative to pH_{SW}. It should be noted that by producing their tubes from a mixture of aragonite and HMC, serpulid worm biomineralization and the resulting $CaCO_3$ matrix is fundamentally different than that of the other marine calcifiers evaluated in this study, which are predominantly monomineralic. To our knowledge, these are the first reported B isotope measurements for serpulid worm tubes and the $\delta^{11}B$ values for this mixed mineralogy precipitating organism is not consistant with significant boric acid incorporation into the carbonate lattice (Fig .5)..

4.2.5 American oyster

The $\delta^{11}B_{CaCO3}$ for the American oyster *C. virginica* evaluated in this study (16.03 ‰; n = 1; Tables 3 and 4) is less than the theoretical value of $\delta^{11}B$ for seawater borate (Fig. 4). Oysters construct their shells of LMC (aragonite during the larval stage) from a discrete calcifying fluid known as the extrapallial fluid ('EPF'; e.g., Crenshaw, 1972), with hemocytes and organic templates playing a potentially important role in crystal nucleation (e.g., Wilbur and Saleuddin 1983; Wheeler 1992; Marie et al., 2012; Weiner et al., 1984; Mount et al., 2004).). The sample of *C. virginica* evaluated in this study was exposed to seawater conditions (pH_{SW} = 8.2; 25 °C; 32 psu; Table 4) that yield a theoretical borate $\delta^{11}B$, and thus $\delta^{11}B_{CaCO3}$, of 19.57 ‰, which is 3.54 ‰ greater than $\delta^{11}B_{CaCO3}$ measured for *C. virginica*. The observation that oyster $\delta^{11}B_{CaCO3}$ is substantially less than theoretical $\delta^{11}B$ of seawater borate suggests that pH_{CF} of oyster extrapallial fluid is less than the pH of the oyster's surrounding seawater. Indeed, pH microelectrode measurements show that pH of oyster EPF (pH_{EPF}) is approximately 0.5 units less than seawater pH, which the author attributes to metabolically driven accumulation of dissolved CO_2 when the oyster's shell is closed (Crenshaw, 1972; Littlewood and Young, 1994; Michaelidis et al., 2005). Oysters appear to overcome low $CaCO_3$ saturation state in the EPF, compared to corals that maintain elevated $CaCO_3$ saturation state at their site of calcification, by using organic templates to facilitate biomineral growth (e.g., Marie et al., 2012; Addadi et al., 2003; Weiner et al., 1984). The oyster could generate this negative divergence in $\delta^{11}B_{CaCO3}$ from seawater borate $\delta^{11}B$ by decreasing pH_{CF} by 0.35 units (Table 4), which, given the proximity of the independent pH-microelectrode measurements of oyster EPF, seems to be a plausible explanation for why oyster $\delta^{11}B_{CaCO3}$ falls below the theoretical borate $\delta^{11}B$-pH curve (Klochko et al., 2009; Fig 5). To our knowledge, these are the first reported B isotope measurements for oysters and the $\delta^{11}B$ values for this low Mg calcite-precipitating organism are not consistant with significant boric acid incorporation into the carbonate lattice (Fig. 5).

4.3 Estimating pH_{CF} from $\delta^{11}B_{CaCO3}$

The 6 species of calcifying marine organisms investigated in the present study exhibited average $\delta^{11}B_{CaCO3}$ compositions ranging from 16.27 ‰ to 35.09 ‰ (Table 3). Given that all 6 species were grown under nearly equivalent controlled laboratory conditions, the large interspecific range in $\delta^{11}B_{CaCO3}$ supports the hypothesis that boron isotope fractionation in marine calcifiers cannot be explained solely by borate incorporation at ambient pH_{SW} (see Table 5 and references therein). We hypothesize that this species-dependent variability is driven by interspecific differences in pH_{CF}. To explore this hypothesis, $\delta^{11}B_{CaCO3}$ values were converted to pH_{CF} from measured seawater temperature, salinity, seawater $\delta^{11}B$ value of 39.61 ± 0.20 ‰ (Foster et al., 2010), and an α of 1.0272 (Klochko et al., 2006; Table 4). In the absence of empirical measurements of calcifying fluid temperature, salinity, and $\delta^{11}B$, these parameters are assumed to reflect seawater. These calculations yield a pH_{CF}, assuming that only borate is incorporated (see Table 4), of 8.5 for the temperate coral (*O. arbuscula*), 9.4 for the coralline red alga (*Neogoniolithion* sp.), 8.1 for the tropical urchin *(E. tribuloides*), 7.9 for the temperate urchin (*A. punctulata*), 8.2 for the serpulid worm (*H. crucigera*), and 7.9 for the American oyster (*C. virginica*).

4.3.1 Sensitivity of $\delta^{11}B_{CaCO3}$-based calculations of pH_{CF} to choice of pK_B and α

Here, we evaluate the sensitivity of calculating pH_{CF} from measured $\delta^{11}B_{CaCO3}$ composition by testing the two principal factors that may influence the theoretical model of borate $\delta^{11}B$ variation as a function of both pH_{CF} and pH_{SW}; namely pK_B and α. A sensitivity analysis of $\delta^{11}B$ in seawater was not conducted since all organisms evaluated in this study were exposed to seawater from the same source and, thus, of identical $\delta^{11}B$ composition.

The determination of pH_{CF} from pK_B, $\delta^{11}B$ of calcifying fluid ($\delta^{11}B_{CF}$), and $\delta^{11}B_{CaCO3}$ can be summarized with the following equation (Eq. 1):

$$pH_{CF} = pK_B - \log((\delta^{11}B_{CF} - \delta^{11}B_{CaCO3})/(\delta^{11}B_{CF} - (\alpha \times \delta^{11}B_{CaCO3}) - 1000(\alpha - 1))); \quad (1)$$

where pK_B is 8.6152 (at 25°C and 32 psu; Dickson, 1990), $\delta^{11}B_{CF}$ is 39.61 ‰ (inherited from $^{11}B_{SW}$; Foster et al., 2010), and
455 α is 1.0272 (Klochko et al., 2006). Thus, $\delta^{11}B_{CaCO3}$, can be calculated across a range of pH_{CF} (Fig. 1b; Table S1).

It is important to note that the difference in $\delta^{11}B_{CaCO3}$ between each pH unit (when fluid pH < pK_B) increases with pH, as shown in Fig. 1b (see also Table S1). For example, a change in pH from 7.75 to 7.80 predicts a $\delta^{11}B_{CaCO3}$ difference of 0.35 ‰ (15.77 ‰ – 15.42 ‰), whereas a change in pH from 8.35 to 8.40 predicts a $\delta^{11}B_{CaCO3}$ difference of 0.74 ‰ (22.59 ‰ – 21.85 ‰). Thus, the relationship between pH_{CF} and $\delta^{11}B_{CaCO3}$ is nonlinear over the range of pH_{CF} of interest (7 < pH < 10),
460 with pH having the greatest influence on $\delta^{11}B_{CaCO3}$, as fluid pH_{CF} approaches pK_B.

As discussed above (section 4.2), most marine calcifiers are thought to precipitate $CaCO_3$ from a discrete 'calcifying fluid', which appears to be derived, yet physically separated, from seawater and with a pH greater than (e.g., coralline alga, corals), equivalent to (e.g., serpulid worm, urchins), or less than (e.g., oysters) seawater. Although the sensitivity analysis for the $\delta^{11}B_{CaCO3}$-derived determinations of pH_{CF} at a pK_B of 8.6152 indicates that a small change in pH_{CF} greatly influences $\delta^{11}B_{CaCO3}$,
465 especially as pH approaches pK_B (8.6152), the range of the organisms' seawater pH (8.0-8.2; Table 4) could only account for a 2.24 ‰ range in $\delta^{11}B_{CaCO3}$ (Table S1), far less than the ca. 20 ‰ range that was observed. It therefore follows that the large variability in $\delta^{11}B_{CaCO3}$ (*ca.* 20 ‰) observed for the investigated species requires an alternative explanation, such as changes in pH_{CF} —particularly for the coralline alga, coral and oyster species that exhibited such large deviations in predicted vs. observed $\delta^{11}B_{CaCO3}$ (see section 4.2).

470 **4.3.2 Sensitivity analysis of δ^{11}B-derived pH_{CF} to α**

As discussed in the Introduction (section 1.1), much work has gone into establishing an α that accurately describes the pH-dependent relationship between $\delta^{11}B$ of dissolved borate and boric acid in seawater (see Xiao et al., 2014, for detailed discussion), with the earliest published palaeo-pH reconstructions using a theoretical value of 1.0194 (Kakihana et al., 1977; see Fig. 2). An empirical α of 1.0272 (Klochko et al., 2006) has now been shown to better predict $\delta^{11}B_{B(OH)4-}$, viz. $\delta^{11}B_{CaCO3}$,
475 across a range of pH relevant for seawater (Rollion-Bard and Erez, 2010; Xiao et al., 2014). However, $\delta^{11}B_{CaCO3}$ of many species of calcifying marine organisms fall either above or below the theoretical $\delta^{11}B_{B(OH)4-}$-pH curves. It has long been suggested (and shown for corals) that calcifying organisms diverge from the predicted $\delta^{11}B_{CaCO3}$ due to their ability to modify pH of their calcifying environments (e.g., Anagnostou et al., 2012; Hönisch et al., 2004; Krief et al., 2010; Rae et al., 2011; Reynaud et al., 2004; Trotter et al., 2011; McCulloch et al., 2012; Wall et al., 2016). In the present study, species-specific
480 divergences in $\delta^{11}B_{CaCO3}$ from the theoretical $\delta^{11}B_{B(OH)4-}$pH curves are interpreted as evidence of the differing capacities of calcifying marine species to modify pH_{CF}. Importantly, existing models of biomineralization for each species are generally compatible with these $\delta^{11}B_{CaCO3}$-derived estimates of pH_{CF} (see section 4.2).

Although an α of 1.0272 (Klochko et al., 2006) was used in the present study to estimate pH_{CF}, other theoretical values for α, yielding slightly different borate $\delta^{11}B$-pH curves (e.g., Byrne et al., 2006; Palmer et al., 1987; see Fig. 4), will yield slightly
485 different estimates of pH_{CF} for each organism. For example, using α values of 1.033 (Palmer et al. 1987), 1.0285 (Byrne et al. 2006), 1.0272 (Klochko et al. 2006), and 1.0194 (Kakihana et al. 1977) and a $\delta^{11}B_{CaCO3}$ of 24.12 ‰ (temperate coral; pH_{SW} = 8.1) yields pH_{CF} of 8.7, 8.6, 8.5, and 8.1, respectively – a difference of 0.6 pH units. It should also be noted that the lower the $\delta^{11}B_{CaCO3}$, the more sensitive the reconstructed pH is to choice of α. For example, changing α from 1.0272 to 1.0330 will

result in a 0.24 pH unit shift for $\delta^{11}B_{CaCO3}$ = 20 ‰, but only a 0.12 and 0.08 pH unit shift for $\delta^{11}B_{CaCO3}$ = 30 ‰ and 39.5 ‰, respectively. This underscores the importance of using the same α when comparing pH_{CF} amongst species.

4.3.3 Implications of $\delta^{11}B_{CaCO3}$-derived estimates of pH_{CF} for species-specific vulnerability to ocean acidification

Understanding how marine organisms calcify is a critical requirement for understanding and, ideally, predicting their physiological responses to future ocean acidification (e.g., Kleypas et al., 2006). Notably, the different species' $\delta^{11}B_{CaCO3}$ and reconstructed pH_{CF} exhibit a moderate, inverse relationship with their experimentally determined vulnerability to ocean acidification (Ries et al., 2009). Species exhibiting more resilient 'parabolic' (e.g., coralline red alga) and 'threshold' (e.g., coral, tropical urchin) responses to ocean acidification generally exhibited a higher $\delta^{11}B_{CaCO3}$ and, thus, pH_{CF} than species exhibiting the more vulnerable 'negative' responses (e.g., oyster, serpulid worm) to ocean acidification (Table 4). The temperate urchin was the exception to this general trend, as it exhibited a relatively resilient parabolic response to ocean acidification yet maintained $\delta^{11}B_{CaCO3}$ and, thus, pH_{CF} close to that of pH_{SW}. These results support the assertion that interspecific differences in pH_{CF} calcification site pH contribute to marine calcifiers' differential responses to ocean acidification – highlighting the need for future queries into the mechanisms driving boron isotope fractionation and biomineralization within marine calcifying organisms.

4.3.4 Further calibration of the $\delta^{11}B_{CaCO3}$-derived determinations of pH

The observed deviations of the investigated species' $\delta^{11}B_{CaCO3}$ from the borate $\delta^{11}B$-pH curve also highlight that, in some species, paleo-seawater pH may not simply be reconstructed by projecting measured $\delta^{11}B_{CaCO3}$ onto a theoretical seawater $\delta^{11}B_{B(OH)4-}$-pH curve (see also Sanyal et al., 1996, Sanyal et al., 2001; Honïsch et al., 2003; Trotter et al., 2011; Anagnostou et al., 2012). Instead, the model species used for paleo-seawater pH reconstructions may require calibration through controlled laboratory experiments and/or core-top calibrations that empirically define the species-specific relationship between seawater pH and $\delta^{11}B_{CaCO3}$.

5 Conclusion

This study establishes the methodology for measuring stable boron isotopes at Ifremer (Plouzané, France) and reveals that neither cleaning protocol (oxidized vs. untreated), nor method of sample preparation (batch vs. column), nor injection system (d-DIHEN vs. ammonia addition) causes a significant difference in $\delta^{11}B_{CaCO3}$ composition of the samples. The batch method of boron extraction is preferred over the column chemistry method since the risk of B contamination is reduced in the batch method due to shorter exposure to potential contaminants and smaller reagent volumes.

This newly established method for measuring stable boron isotopes at Ifremer was used to measure the $\delta^{11}B_{CaCO3}$ composition of six species of marine calcifiers that were all grown under equivalent seawater conditions. The coralline red alga *Neogoniolithion* sp. (35.89 ± 3.71 ‰; n = 3) exhibited the highest $\delta^{11}B_{CaCO3}$, followed by the temperate coral *O. arbuscula* (24.12 ± 0.19 ‰; n = 3), the tube of the serpulid worm *H. crucigera* (19.26 ± 0.16 ‰; n = 3), the tropical urchin *E. tribuloides* (18.71 ± 0.26 ‰; n = 3), the temperate urchin *A. punctulata* (16.28 ± 0.86 ‰; n = 3), and the American oyster *C. virginica* (16.03 ‰; n = 1). The observed *ca.* 20 ‰ range in $\delta^{11}B_{CaCO3}$ composition of the investigated species constitutes the largest range in biogenic $\delta^{11}B_{CaCO3}$ reported to date.

Consideration of these extreme interspecific differences in $\delta^{11}B_{CaCO3}$ in the context of existing models of biomineralization for the investigated species, combined with published measurements of pH_{CF} for some of the species, generally supports the assertion that most marine calcifiers precipitate their $CaCO_3$ from a discrete calcifying medium with a pH that is either greater

than, equivalent to, or, for some species, less than external seawater pH. Furthermore, the observation that the different species' $\delta^{11}B_{CaCO3}$ and reconstructed pH_{CF} generally varied inversely with their experimentally determined vulnerability to ocean acidification suggests that a species' relative resilience (or vulnerability) to OA may be influenced by their ability (or lack thereof) to maintain an elevated pH_{CF}. These observations contribute to the growing body of work that uses $\delta^{11}B_{CaCO3}$ as a tool to advance understanding of the mechanisms by which marine calcifiers build and maintain their shells and skeletons and, ultimately, how they will respond to anthropogenic ocean acidification.

References

Addadi, L., Raz, S. and Weiner, S.: Taking Advantage of Disorder: Amorphous Calcium Carbonate and Its Roles in Biomineralization, Adv. Mater., 15(12), 959–970, doi:10.1002/adma.200300381, 2003.

Al-Ammar, A. S., Gupta, R. K. and Barnes, R. M.: Elimination of boron memory effect in inductively coupled plasma-mass spectrometry by ammonia gas injection into the spray chamber during analysis, Spectrochim. Acta Part B At. Spectrosc., 55(6), 629–635, doi:10.1016/S0584-8547(00)00197-X, 2000.

Al-Horani, F. A., Al-Moghrabi, S. M. and de Beer, D.: The mechanism of calcification and its relation to photosynthesis and respiration in the scleractinian coral Galaxea fascicularis, Mar. Biol., 142(3), 419–426, doi:10.1007/s00227-002-0981-8, 2003.

Allison, N. and Finch, A. A.: δ11B, Sr, Mg and B in a modern Porites coral: the relationship between calcification site pH and skeletal chemistry, Geochim. Cosmochim. Acta, 74(6), 1790–1800, doi:10.1016/j.gca.2009.12.030, 2010.

Ameye, L., Compère, P., Dille, J. and Dubois, P.: Ultrastructure and cytochemistry of the early calcification site and of its mineralization organic matrix in Paracentrotus lividus (Echinodermata: Echinoidea), Histochem. Cell Biol., 110(3), 285–294, doi:10.1007/s004180050290, 1998.

Anagnostou, E., Huang, K.-F., You, C.-F., Sikes, E. L. and Sherrell, R. M.: Evaluation of boron isotope ratio as a pH proxy in the deep sea coral Desmophyllum dianthus: Evidence of physiological pH adjustment, Earth Planet. Sci. Lett., 349–350, 251–260, doi:10.1016/j.epsl.2012.07.006, 2012.

Balan, E., Pietrucci, F., Gervais, C., Blanchard, M., Schott, J. and Gaillardet, J.: First-principles study of boron speciation in calcite and aragonite, Geochim. Cosmochim. Acta, 193, doi:10.1016/j.gca.2016.07.026, 2016.

Barker, S., Greaves, M. and Elderfield, H.: A study of cleaning procedures used for foraminiferal Mg/Ca paleothermometry, Geochemistry, Geophys. Geosystems, 4(9), 1–20, doi:10.1029/2003GC000559, 2003.

Bates, N. R.: Interannual variability of the oceanic CO2 sink in the subtropical gyre of the North Atlantic Ocean over the last 2 decades, J. Geophys. Res. Ocean., 112(9), 1–26, doi:10.1029/2006JC003759, 2007.

Bartoli, G., Hönisch, B. and Zeebe, R. E.: Atmospheric CO 2 decline during the Pliocene intensification of Northern Hemisphere glaciations, Paleoceanography, 26(4), doi:10.1029/2010PA002055, 2011.

Borowitzka, M. A. and Larkum, A. W. D.: Calcification in algae: Mechanisms and the role of metabolism, CRC. Crit. Rev. Plant Sci., 6(1), 1–45, doi:10.1080/07352688709382246, 1987.

Byrne, R. H., Yao, W., Klochko, K., Tossell, J. A. and Kaufman, A. J.: Experimental evaluation of the isotopic exchange equilibrium 10B(OH)3+11B(OH)4−=11B(OH)3+10B(OH)4− in aqueous solution, Deep Sea Res. Part I Oceanogr. Res. Pap., 53(4), 684–688, doi:10.1016/j.dsr.2006.01.005, 2006.

Byrne, R. H., Mecking, S., Feely, R. A. and Liu, X.: Direct observations of basin-wide acidification of the North Pacific Ocean, Geophys. Res. Lett., 37(2), 1–5, doi:10.1029/2009GL040999, 2010.

Cameron, J. N.: Post-Moult Calcification in the Blue Crab (Callinectes Sapidus): Relationships between Apparent Net H+ Excretion, Calcium and Bicarbonate, J. Exp. Biol., 119(1), 275 LP-285 [online] Available from: http://jeb.biologists.org/content/119/1/275.abstract, 1985.

Catanzaro, E. J., Champion, C. E., Garner, E. L., Marinenko, G., Sappenfield, K. . and Shields, W. R.: Boric acid: Isotopic and assay standard reference materials, US National Bureau of Standards, Special Publication, 260-17., 1970.

Cohen, A. and Holcomb, M.: Why Corals Care About Ocean Acidification: Uncovering the Mechanism, Oceanography, 22(4), 118–127, doi:10.5670/oceanog.2009.102, 2009.

Cohen, A. L. and McConnaughey, T. A.: Geochemical Perspectives on Coral Mineralization, in Biomineralization, edited by P. M. Dove, J. J. De Yoreo, and S. Weiner, pp. 151–188, Mineralogical Society of America Geochemical Society., 2003.

Crenshaw, M. A.: The Inorganic Composition of Molluscan Extrapallial Fluid, Biol. Bull., 143(3), 506–512, doi:10.2307/1540180, 1972.

Cuif, J. P. and Dauphin, Y.: The Environment Recording Unit in coral skeletons – a synthesis of structural and chemical evidences for a biochemically driven, stepping-growth process in fibres, Biogeosciences, 2(1), 61–73, doi:10.5194/bg-2-61-2005, 2005.

Cusack, M., Kamenos, N. A., Rollion-Bard, C. and Tricot, G.: Red coralline algae assessed as marine pH proxies using 11B MAS NMR, Sci. Rep., 5, 8175, doi:10.1038/srep08175, 2015.

D'Olivo, J. P., McCulloch, M. T., Eggins, S. M. and Trotter, J.: Coral records of reef-water pH across the central Great Barrier Reef, Australia: assessing the influence of river runoff on inshore reefs, Biogeosciences, 12(4), 1223–1236, doi:10.5194/bg-12-1223-2015, 2015.

Dickson, A. G.: Thermodynamics of the dissociation of boric acid in synthetic seawater from 273.15 to 318.15 K, Deep Sea Res. Part A. Oceanogr. Res. Pap., 37(5), 755–766, doi:10.1016/0198-0149(90)90004-F, 1990.

Dishon, G., Fisch, J., Horn, I., Kaczmarek, K., Bijma, J., Gruber, D. F., Nir, O., Popovich, Y. and Tchernov, D.: A novel paleo-bleaching proxy using boron isotopes and high-resolution laser ablation to reconstruct coral bleaching events, Biogeosciences, 12(19), 5677–5687, doi:10.5194/bg-12-5677-2015, 2015.

Dissard, D., Douville, E., Reynaud, S., Juillet-Leclerc, A., Montagna, P., Louvat, P. and McCulloch, M.: Light and temperature effects on δ11B and B / Ca ratios of the zooxanthellate coral Acropora sp.: results from culturing experiments, Biogeosciences, 9(11), 4589–4605, doi:10.5194/bg-9-4589-2012, 2012.

Doney, S. C., Fabry, V. J., Feely, R. A. and Kleypas, J. A.: Ocean Acidification: The Other CO 2Problem, Ann. Rev. Mar. Sci., 1(1), 169–192, doi:10.1146/annurev.marine.010908.163834, 2009.

Dore, J. E., Lukas, R., Sadler, D. W., Church, M. J. and Karl, D. M.: Physical and biogeochemical modulation of ocean acidification in the central North Pacific, Proc. Natl. Acad. Sci., 106(30), 12235–12240, doi:10.1073/pnas.0906044106, 2009.

Douville, E., Paterne, M., Cabioch, G., Louvat, P., Gaillardet, J., Juillet-Leclerc, A. and Ayliffe, L.: Abrupt sea surface pH change at the end of the Younger Dryas in the central sub-equatorial Pacific inferred from boron isotope abundance in corals (Porites), Biogeosciences, 7(8), 2445–2459, doi:10.5194/bg-7-2445-2010, 2010.

Fabry, V. J., Seibel, B. A., Feely, R. A. and Orr, J. C.: Impacts of ocean acidification on marine fauna and ecosystem processes, ICES J. Mar. Sci., 65(Dic), 414–432, 2008.

Farmer, J. R., Hönisch, B., Robinson, L. F. and Hill, T. M.: Effects of seawater-pH and biomineralization on the boron isotopic composition of deep-sea bamboo corals, Geochim. Cosmochim. Acta, 155, 86–106, doi:10.1016/j.gca.2015.01.018, 2015.

Feely, R. A., Sabine, C. L., Hernandez-Ayon, J. M., Ianson, D. and Hales, B.: Evidence for Upwelling of Corrosive "Acidified" Water onto the Continental Shelf, Science (80-.)., 320(5882), 1490–1492, doi:10.1126/science.1155676, 2008.

Foster, G. L.: Seawater pH, pCO2 and [CO2-3] variations in the Caribbean Sea over the last 130??kyr: A boron isotope and B/Ca study of planktic foraminifera, Earth Planet. Sci. Lett., 271(1–4), 254–266, doi:10.1016/j.epsl.2008.04.015, 2008.

Foster, G. L. and Sexton, P. F.: Enhanced carbon dioxide outgassing from the eastern equatorial Atlantic during the last glacial, Geology, 42(11), 1003–1006, doi:10.1130/G35806.1, 2014.

Foster, G. L., Pogge Von Strandmann, P. A. E. and Rae, J. W. B.: Boron and magnesium isotopic composition of seawater, Geochemistry, Geophys. Geosystems, 11(8), 1–10, doi:10.1029/2010GC003201, 2010.

Foster, G. L., Lear, C. H. and Rae, J. W. B.: The evolution of pCO2, ice volume and climate during the middle Miocene, Earth Planet. Sci. Lett., 341–344, 243–254, doi:10.1016/j.epsl.2012.06.007, 2012.

Foster, G. L., Hönisch, B., Paris, G., Dwyer, G. S., Rae, J. W. B., Elliott, T., Gaillardet, J., Hemming, N. G., Louvat, P. and Vengosh, A.: Interlaboratory comparison of boron isotope analyses of boric acid, seawater and marine CaCO3 by MC-ICPMS and NTIMS, Chem. Geol., 358, 1–14, doi:10.1016/j.chemgeo.2013.08.027, 2013.

Gaetani, G. A. and Cohen, A. L.: Element partitioning during precipitation of aragonite from seawater: A framework for understanding paleoproxies, Geochim. Cosmochim. Acta, 70(18), 4617–4634, doi:10.1016/j.gca.2006.07.008, 2006.

Gaillardet, J. and Allègre, C. J.: Boron isotopic compositions of corals: Seawater or diagenesis record?, Earth Planet. Sci. Lett., 136(3–4), 665–676, doi:10.1016/0012-821X(95)00180-K, 1995.

Goldberg, W. M.: Desmocytes in the calicoblastic epithelium of the stony coral Mycetophyllia reesi and their attachment to the skeleton, Tissue Cell, 33(4), 388–394, doi:10.1054/tice.2001.0192, 2001.

González-Dávila, M., Santana Casiano, J. M. and Machín, F.: Changes in the partial pressure of carbon dioxide in the Mauritanian-Cape Verde upwelling region between 2005 and 2012, Biogeosciences Discuss., 2, 1–31, doi:10.5194/bg-2017-

83, 2017.

Hedley, R. H.: Studies of Serpulid Tube Formation. I. The secretion of the Calcareous and Organic Components of the Tube by Pomatoceros triqueter., Quaterly Journval Microsc. Sci., 97(September), 411–419, 1956.

Heinemann, A., Fietzke, J., Melzner, F., Böhm, F., Thomsen, J., Garbe-Schnberg, D. and Eisenhauer, A.: Conditions of Mytilus edulis extracellular body fluids and shell composition in a pH-treatment experiment: Acid-base status, trace elements and $\delta^{11}B$, Geochemistry, Geophys. Geosystems, 13(1), doi:10.1029/2011GC003790, 2012.

Hemming, N. G. and Hanson, G. N.: Boron isotopic composition and concentration in modern marine carbonates, Geochim. Cosmochim. Acta, 56(1), 537–543, doi:10.1016/0016-7037(92)90151-8, 1992.

Hemming, N. G. and Hönisch, B.: Chapter Seventeen Boron Isotopes in Marine Carbonate Sediments and the pH of the Ocean, in Developments in Marine Geology, vol. 1, pp. 717–734., 2007.

Hemming, N. G., Guilderson, T. P. and Fairbanks, R. G.: Seasonal variations in the boron isotopic composition of coral: A productivity signal?, Global Biogeochem. Cycles, 12(4), 581–586, doi:10.1029/98GB02337, 1998.

Holcomb, M., McCorkle, D. C. and Cohen, A. L.: Long-term effects of nutrient and CO2 enrichment on the temperate coral Astrangia poculata (Ellis and Solander, 1786), J. Exp. Mar. Bio. Ecol., 386(1–2), 27–33, doi:10.1016/j.jembe.2010.02.007, 2010.

Holcomb, M., Venn, A. A., Tambutté, E., Tambutté, S., Allemand, D., Trotter, J. and McCulloch, M.: Coral calcifying fluid pH dictates response to ocean acidification, Sci. Rep., 4, doi:10.1038/srep05207, 2014.

Hönisch, B., Bijma, J., Russell, A. ., Spero, H., Palmer, M. R., Zeebe, R. E. and Eisenhauer, A.: The influence of symbiont photosynthesis on the boron isotopic composition of foraminifera shells, Mar. Micropaleontol., 49(1–2), 87–96, doi:10.1016/S0377-8398(03)00030-6, 2003.

Hönisch, B. and Hemming, N. G.: Ground-truthing the boron isotope-paleo-pH proxy in planktonic foraminifera shells: Partial dissolution and shell size effects, Paleoceanography, 19(4), n/a-n/a, doi:10.1029/2004PA001026, 2004.

Hönisch, B. and Hemming, N. G.: Surface ocean pH response to variations in pCO2 through two full glacial cycles, Earth Planet. Sci. Lett., 236(1–2), 305–314, doi:10.1016/j.epsl.2005.04.027, 2005.

Hönisch, B., Hemming, N. G., Grottoli, A. G., Amat, A., Hanson, G. N. and Bijma, J.: Assessing scleractinian corals as recorders for paleo-pH: Empirical calibration and vital effects, Geochim. Cosmochim. Acta, 68(18), 3675–3685, doi:10.1016/j.gca.2004.03.002, 2004.

Hönisch, B., Hemming, N. G., Archer, D., Siddall, M. and McManus, J. F.: Atmospheric carbon dioxide concentration across the mid-Pleistocene transition., Science, 324(5934), 1551–4, doi:10.1126/science.1171477, 2009.

IPCC: Climate Change 2013 - The Physical Science Basis, edited by Intergovernmental Panel on Climate Change, Cambridge University Press, Cambridge., 2014.

Jorgensen, B. B., Erez, J., Revsbech, N. P. and Cohen, Y.: Symbiotic photosynthesis in a planktonic foraminifera, Globigerinoides sacculifer (Brady), studied with microelectrodes, Limnol. Oceanogr.., 30(6), 1253–1267, 1985.

Kaczmarek, K., Langer, G., Nehrke, G., Horn, I., Misra, S., Janse, M. and Bijma, J.: Boron incorporation in the foraminifer Amphistegina lessonii under a decoupled carbonate chemistry, Biogeosciences, 12(6), 1753–1763, doi:10.5194/bg-12-1753-2015, 2015.

Kakihana, H., Kotaka, M., Satoh, S., Nomura, M. and Okamoto, M.: Fundamental Studies on the Ion-Exchange Separation of Boron Isotopes, Bull. Chem. Soc. Jpn., 50(1), 158–163, doi:10.1246/bcsj.50.158, 1977.

Kasemann, S. A., Schmidt, D. N., Bijma, J. and Foster, G. L.: In situ boron isotope analysis in marine carbonates and its application for foraminifera and palaeo-pH, Chem. Geol., 260(1–2), 138–147, doi:10.1016/j.chemgeo.2008.12.015, 2009.

Kiss, E.: Ion-exchange separation and spectrophotometric determination of boron in geological materials, Anal. Chim. Acta, 211, 243–256, doi:10.1016/S0003-2670(00)83684-3, 1988.

Kleypas, J. A., Feely, R. A., Fabry, V. J., Langdon, C., Sabine, C. L. and Robbins, L. L.: Impacts of ocean acidification on coral reefs and other marine calcifiers. A guide for future research., 2006.

Klochko, K., Kaufman, A. J., Yao, W., Byrne, R. H. and Tossell, J. A.: Experimental measurement of boron isotope fractionation in seawater, Earth Planet. Sci. Lett., 248(1–2), 276–285, doi:10.1016/j.epsl.2006.05.034, 2006.

Klochko, K., Cody, G. D., Tossell, J. A., Dera, P. and Kaufman, A. J.: Re-evaluating boron speciation in biogenic calcite and aragonite using 11B MAS NMR, Geochim. Cosmochim. Acta, 73(7), 1890–1900, doi:10.1016/j.gca.2009.01.002, 2009.

Krief, S., Hendy, E. J., Fine, M., Yam, R., Meibom, A., Foster, G. L. and Shemesh, A.: Physiological and isotopic responses of scleractinian corals to ocean acidification, Geochim. Cosmochim. Acta, 74(17), 4988–5001, doi:10.1016/j.gca.2010.05.023, 2010.

Kroeker, K. J., Kordas, R. L., Crim, R. N. and Singh, G. G.: Meta-analysis reveals negative yet variable effects of ocean acidification on marine organisms, Ecol. Lett., 13(11), 1419–1434, doi:10.1111/j.1461-0248.2010.01518.x, 2010.

Kroeker, K. J., Kordas, R. L., Crim, R., Hendriks, I. E., Ramajo, L., Singh, G. S., Duarte, C. M. and Gattuso, J. P.: Impacts of ocean acidification on marine organisms: Quantifying sensitivities and interaction with warming, Glob. Chang. Biol., 19(6), 1884–1896, doi:10.1111/gcb.12179, 2013.

Kubota, K., Yokoyama, Y., Ishikawa, T., Obrochta, S. and Suzuki, A.: Larger CO2 source at the equatorial Pacific during the last deglaciation., Sci. Rep., 4, 5261, doi:10.1038/srep05261, 2014.

Langdon, C.: Review of experimental evidence for effects of CO2 on calcification of reef builders., in Proc. 9th Int. Coral Reef Sym, pp. 1–8. [online] Available from: http://people.uncw.edu/szmanta/2006 pdfs/20 Global warming issues/Langdon 9I CRSProceedings CO2 calcification.pdf, 2002.

Lee, D. and Carpenter, S. J.: Isotopic disequilibrium in marine calcareous algae, Chem. Geol., 172(3–4), 307–329, doi:10.1016/S0009-2541(00)00258-8, 2001.

Lemarchand, D., Gaillardet, J., Lewin, É. and Allègre, C. J.: The influence of rivers on marine boron isotopes and implications for reconstructing past ocean pH, Nature, 408(6815), 951–954, doi:10.1038/35050058, 2000.

Lemarchand, D., Gaillardet, J., Göpel, C. and Manhès, G.: An optimized procedure for boron separation and mass spectrometry analysis for river samples, Chem. Geol., 182(2–4), 323–334, doi:10.1016/S0009-2541(01)00329-1, 2002.

Littlewood, D. T. J. and Young, R. E.: The effect of air-gaping behaviour on extrapallial fluid pH in the tropical oyster Crassostrea rhizophorae, Comp. Biochem. Physiol. Part A Physiol., 107(1), 1–6, doi:10.1016/0300-9629(94)90264-X, 1994.

Liu, Y. and Tossell, J. A.: Ab initio molecular orbital calculations for boron isotope fractionations on boric acids and borates, Geochim. Cosmochim. Acta, 69(16), 3995–4006, doi:10.1016/j.gca.2005.04.009, 2005.

Liu, Y., Liu, W., Peng, Z., Xiao, Y., Wei, G., Sun, W., He, J., Liu, G. and Chou, C. L.: Instability of seawater pH in the South China Sea during the mid-late Holocene: Evidence from boron isotopic composition of corals, Geochim. Cosmochim. Acta, 73(5), 1264–1272, doi:10.1016/j.gca.2008.11.034, 2009.

Louvat, P., Bouchez, J. and Paris, G.: MC-ICP-MS Isotope Measurements with Direct Injection Nebulisation (d-DIHEN): Optimisation and Application to Boron in Seawater and Carbonate Samples, Geostand. Geoanalytical Res., 35(1), 75–88, doi:10.1111/j.1751-908X.2010.00057.x, 2011.

Louvat, P., Moureau, J., Paris, G., Bouchez, J., Noireaux, J. and Gaillardet, J. J. J.: A fully automated direct injection nebulizer (d-DIHEN) for MC-ICP-MS isotope analysis: application to boron isotope ratio measurements, J. Anal. At. Spectrom., 29(9), doi:10.1039/C4JA00098F, 2014.

Marie, B., Joubert, C., Tayale, A., Zanella-Cleon, I., Belliard, C., Piquemal, D., Cochennec-Laureau, N., Marin, F., Gueguen, Y. and Montagnani, C.: Different secretory repertoires control the biomineralization processes of prism and nacre deposition of the pearl oyster shell, Proc. Natl. Acad. Sci., 109(51), 20986–20991, doi:10.1073/pnas.1210552109, 2012.

Martin, P., Goodkin, N. F., Stewart, J. A., Foster, G. L., Sikes, E. L., White, H. K., Hennige, S. and Roberts, J. M.: Deep-sea coral δ13C: A tool to reconstruct the difference between seawater pH and δ11B-derived calcifying fluid pH, Geophys. Res. Lett., 43, 299–308, doi:10.1002/2015GL066494, 2016.

Martínez-Botí, M. a., Foster, G. L., Chalk, T. B., Rohling, E. J., Sexton, P. F., Lunt, D. J., Pancost, R. D., Badger, M. P. S. and Schmidt, D. N.: Plio-Pleistocene climate sensitivity evaluated using high-resolution CO2 records, Nature, 518(7537), 49–54, doi:10.1038/nature14145, 2015a.

Martínez-Botí, M. A., Marino, G., Foster, G. L., Ziveri, P., Henehan, M. J., Rae, J. W. B., Mortyn, P. G. and Vance, D.: Boron

isotope evidence for oceanic carbon dioxide leakage during the last deglaciation, Nature, 518, 219–222, doi:10.1038/nature14155, 2015b.

McConnaughey, T.: 13C and 18O isotopic disequilibrium in biological carbonates: I. Patterns, Geochim. Cosmochim. Acta, 53(1), 151–162, doi:10.1016/0016-7037(89)90282-2, 1989.

McConnaughey, T. A. and Falk, R. H.: Calcium-Proton Exchange during Algal Calcification, Biol. Bull., 180(1), 185–195, doi:10.2307/1542440, 1991.

McConnaughey, T. A. and Whelan, J. F.: Calcification generates protons for nutrient and bicarbonate uptake, Earth-Science Rev., 42(1–2), 95–117, doi:10.1016/S0012-8252(96)00036-0, 1997.

McCulloch, M., Falter, J., Trotter, J. and Montagna, P.: Coral resilience to ocean acidification and global warming through pH up-regulation, Nat. Clim. Chang., 2(8), 623–627, doi:10.1038/nclimate1473, 2012.

McCulloch, M. T., Holcomb, M., Rankenburg, K. and Trotter, J. A.: Rapid, high-precision measurements of boron isotopic compositions in marine carbonates, Rapid Commun. Mass Spectrom., 28(24), 2704–2712, doi:10.1002/rcm.7065, 2014.

Meibom, A., Cuif, J. P., Houlbreque, F., Mostefaoui, S., Dauphin, Y., Meibom, K. L. and Dunbar, R.: Compositional variations at ultra-structure length scales in coral skeleton, Geochim. Cosmochim. Acta, 72(6), 1555–1569, doi:10.1016/j.gca.2008.01.009, 2008.

Michaelidis, B., Haas, D. and Grieshaber, M. K.: Extracellular and Intracellular Acid-Base Status with Regard to the Energy Metabolism in the Oyster Crassostrea gigas during Exposure to Air, Physiol. Biochem. Zool., 78(3), 373–383, doi:10.1086/430223, 2005.

Montagna, P., McCulloch, M., Mazzoli, C., Silenzi, S. and Odorico, R.: The non-tropical coral Cladocora caespitosa as the new climate archive for the Mediterranean: high-resolution (~weekly) trace element systematics, Quat. Sci. Rev., 26(3–4), 441–462, doi:10.1016/j.quascirev.2006.09.008, 2007.

Mount, A. S., Wheeler, a P., Paradkar, R. P. and Snider, D.: Hemocyte-mediated shell mineralization in the eastern oyster., Science, 304(5668), 297–300, doi:10.1126/science.1090506, 2004.

Ni, Y., Foster, G. L., Bailey, T., Elliott, T., Schmidt, D. N., Pearson, P., Haley, B. and Coath, C.: A core top assessment of proxies for the ocean carbonate system in surface-dwelling foraminifers, Paleoceanography, 22(3), doi:10.1029/2006PA001337, 2007.

Nir, O., Vengosh, A., Harkness, J. S., Dwyer, G. S. and Lahav, O.: Direct measurement of the boron isotope fractionation factor: Reducing the uncertainty in reconstructing ocean paleo-pH, Earth Planet. Sci. Lett., 414, 1–5, doi:10.1016/j.epsl.2015.01.006, 2015.

Noireaux, J., Mavromatis, V., Gaillardet, J., Schott, J., Montouillout, V., Louvat, P., Rollion-Bard, C. and Neuville, D. R.: Crystallographic control on the boron isotope paleo-pH proxy, Earth Planet. Sci. Lett., 430(November 2015), 398–407, doi:10.1016/j.epsl.2015.07.063, 2015.

Pagani, M., Lemarchand, D., Spivack, A. and Gaillardet, J.: A critical evaluation of the boron isotope-pH proxy: The accuracy of ancient ocean pH estimates, Geochim. Cosmochim. Acta, 69(4), 953–961, doi:10.1016/j.gca.2004.07.029, 2005.

Palmer, M. R.: Reconstructing Past Ocean pH-Depth Profiles, Science (80-.)., 282(5393), 1468–1471, doi:10.1126/science.282.5393.1468, 1998.

Palmer, M. R., Spivack, A. J. and Edmond, J. M.: Temperature and pH controls over isotopic fractionation during absorption of boron marine clay., Geochim. Cosmochim. Acta., 51(9), 2319–2323, doi:http://dx.doi.org/10.1016/0016-7037(87)90285-7, 1987.

Palmer, M. R., Brummer, G. J., Cooper, M. J., Elderfield, H., Greaves, M. J., Reichart, G. J., Schouten, S. and Yu, J. M.: Multi-proxy reconstruction of surface water pCO2 in the northern Arabian Sea since 29ka, Earth Planet. Sci. Lett., 295(1–2), 49–57, doi:10.1016/j.epsl.2010.03.023, 2010.

Pearson, P. and Palmer, M.: Middle eocene seawater pH and atmospheric carbon dioxide concentrations, Science, 284(5421), 1824–6 [online] Available from: http://www.ncbi.nlm.nih.gov/pubmed/10364552, 1999.

Pearson, P. N. and Palmer, M. R.: Atmospheric carbon dioxide concentrations over the past 60 million years , Nature, 406(6797), 695–699 [online] Available from: http://dx.doi.org/10.1038/35021000, 2000.

Pearson, P. N., Foster, G. L. and Wade, B. S.: Atmospheric carbon dioxide through the Eocene–Oligocene climate transition, Nature, 461(7267), 1110–1113 [online] Available from: http://dx.doi.org/10.1038/nature08447, 2009.

Penman, D. and Hönisch, B.: Rapid and sustained surface ocean acidification during the Paleocene-Eocene Thermal Maximum, Paleoceanography, 1–13, doi:10.1002/2014PA002621.Received, 2014.

Rae, J. W. B., Foster, G. L., Schmidt, D. N. and Elliott, T.: Boron isotopes and B/Ca in benthic foraminifera: Proxies for the deep ocean carbonate system, Earth Planet. Sci. Lett., 302(3–4), 403–413, doi:10.1016/j.epsl.2010.12.034, 2011.

Rae, J. W. B., Sarnthein, M., Foster, G. L., Ridgwell, A., Grootes, P. M. and Elliott, T.: Deep water formation in the North Pacific and deglacial CO 2 rise, Paleoceanography, 29(6), 645–667, doi:10.1002/2013PA002570, 2014.

Reynaud, S., Hemming, N. G., Juillet-Leclerc, A. and Gattuso, J. P.: Effect of pCO2 and temperature on the boron isotopic composition of the zooxanthellate coral Acropora sp., Coral Reefs, 23(4), 539–546, doi:10.1007/s00338-004-0399-5, 2004.

Ries, J. B.: A physicochemical framework for interpreting the biological calcification response to CO2-induced ocean acidification, Geochim. Cosmochim. Acta, 75(14), 4053–4064, doi:10.1016/j.gca.2011.04.025, 2011a.

Ries, J. B.: Skeletal mineralogy in a high-CO2 world, J. Exp. Mar. Bio. Ecol., 403(1–2), 54–64, doi:10.1016/j.jembe.2011.04.006, 2011b.

Ries, J. B., Cohen, A. L. and McCorkle, D. C.: Marine calcifiers exhibit mixed responses to CO2-induced ocean acidification, Geology, 37(12), 1131–1134, doi:10.1130/G30210A.1, 2009.

Rink, S., Kühl, M., Bijma, J. and Spero, H. J.: Microsensor studies of photosynthesis and respiration in the symbiotic foraminifer Orbulina universa, Mar. Biol., 131(4), 583–595, doi:10.1007/s002270050350, 1998.

Rollion-Bard, C., Chaussidon, M. and France-lanord, C.: pH control on oxygen isotopic composition of symbiotic corals, Earth Planet. Sci. Lett., 215, 275–288, doi:10.1016/S0012-821X(03)00391-1, 2003.

Rollion-Bard, C. and Erez, J.: Intra-shell boron isotope ratios in the symbiont-bearing benthic foraminiferan Amphistegina lobifera: Implications for ??11B vital effects and paleo-pH reconstructions, Geochim. Cosmochim. Acta, 74(5), 1530–1536, doi:10.1016/j.gca.2009.11.017, 2010.

Rollion-Bard, C., Chaussidon, M. and France-Lanord, C.: Biological control of internal pH in scleractinian corals: Implications on paleo-pH and paleo-temperature reconstructions, Comptes Rendus - Geosci., 343(6), 397–405, doi:10.1016/j.crte.2011.05.003, 2011a.

Rollion-Bard, C., Blamart, D., Trebosc, J., Tricot, G., Mussi, A. and Cuif, J. P.: Boron isotopes as pH proxy: A new look at boron speciation in deep-sea corals using 11B MAS NMR and EELS, Geochim. Cosmochim. Acta, 75(4), 1003–1012, doi:10.1016/j.gca.2010.11.023, 2011b.

Rustad, J. R. and Bylaska, E. J.: Ab Initio Calculation of Isotopic Fractionation in B(OH)3 (aq) and BOH4- (aq), J. Am. Chem. Soc., 129(8), 2222–2223, doi:10.1021/ja0683335, 2007.

Sanyal, A., Hemming, N. G., Hanson, G. N. and Broecker, W. S.: Evidence for a higher pH in the glacial ocean from boron isotopes in foraminifera, Nature, 373(6511), 234–236, doi:10.1038/373234a0, 1995.

Sanyal, A., Hemming, N. G., Broecker, W., Lea, W., Spero, J. and Hanson, N.: Oceanic pH control on the boron isotopic composition of foraminifera : Evidence from culture experiments, Palaeoceanography, 11(5), 513–517, 1996.

Sanyal, A., Hemming, N. G., Broecker, W. S. and Hanson, G. N.: Changes in pH in the eastern equatorial Pacific across stage 5-6 boundary based on boron isotopes in foraminifera, Global Biogeochem. Cycles, 11(1), 125–133, doi:10.1029/97GB00223, 1997.

Sanyal, A., Nugent, M., Reeder, R. J. and Bijma, J.: Seawater pH control on the boron isotopic composition of calcite: evidence from inorganic calcite precipitation experiments, Geochim. Cosmochim. Acta, 64(9), 1551–1555, doi:10.1016/S0016-7037(99)00437-8, 2000.

Sanyal, A., Bijma, J., Spero, H. and Lea, D. W.: Empirical relationship between pH and the boron isotopic composition of Globigerinoides sacculifer : Implications for the boron isotope paleo-pH proxy, Paleoceanography, 16(5), 515–519, doi:10.1029/2000PA000547, 2001.

Schoepf, V., McCulloch, M. T., Warner, M. E., Levas, S. J., Matsui, Y., Aschaffenburg, M. D. and Grottoli, A. G.: Short-

Term Coral Bleaching Is Not Recorded by Skeletal Boron Isotopes, edited by C. R. Voolstra, PLoS One, 9(11), e112011, doi:10.1371/journal.pone.0112011, 2014.

Short, J. A., Pedersen, O. and Kendrick, G. A.: Turf algal epiphytes metabolically induce local pH increase, with implications for underlying coralline algae under ocean acidification, Estuar. Coast. Shelf Sci., 164, 463–470, doi:10.1016/j.ecss.2015.08.006, 2015.

Simkiss, K. and Wilbur, K. M.: Biomineralization: Cell Biology and Miberal Deposition, Academic Press, San Diego., 1989.

Spivak, A. J. (Scripps), You, C.-F. and Smith, J.: Spivack et al 1993.pdf, Nature, 363(may 13), 149–151, 1993.

Stumpp, M., Hu, M. Y., Melzner, F., Gutowska, M. A. and Dorey, N.: Acidified seawater impacts sea urchin larvae pH regulatory systems relevant for calcification, , doi:10.1073/pnas.1209174109/-/DCSupplemental.www.pnas.org/cgi/doi/10.1073/pnas.1209174109, 2012.

Tambutté, E., Allemand, D., Zoccola, D., Meibom, A., Lotto, S., Caminiti, N. and Tambutté, S.: Observations of the tissue-skeleton interface in the scleractinian coral Stylophora pistillata, Coral Reefs, 26(3), 517–529, doi:10.1007/s00338-007-0263-5, 2007.

Trotter, J., Montagna, P., McCulloch, M., Silenzi, S., Reynaud, S., Mortimer, G., Martin, S., Ferrier-Pagès, C., Gattuso, J. P. and Rodolfo-Metalpa, R.: Quantifying the pH "vital effect" in the temperate zooxanthellate coral Cladocora caespitosa: Validation of the boron seawater pH proxy, Earth Planet. Sci. Lett., 303(3–4), 163–173, doi:10.1016/j.epsl.2011.01.030, 2011.

Uchikawa, J., Penman, D. E., Zachos, J. C. and Zeebe, R. E.: Experimental evidence for kinetic effects on B/Ca in synthetic calcite: Implications for potential B(OH)4- and B(OH)3 incorporation, Geochim. Cosmochim. Acta, 150, doi:10.1016/j.gca.2014.11.022, 2015.Vengosh, A., Kolodny, Y., Starinsky, A., Chivas, A. R. and McCulloch, M. T.: Coprecipitation and isotopic fractionation of boron in modern biogenic carbonates, Geochim. Cosmochim. Acta, 55(10), 2901–2910, doi:10.1016/0016-7037(91)90455-E, 1991.

Venn, A., Tambutté, E., Holcomb, M., Allemand, D. and Tambutté, S.: Live tissue imaging shows reef corals elevate pH under their calcifying tissue relative to seawater, PLoS One, 6(5), doi:10.1371/journal.pone.0020013, 2011.

Venn, A. A., Tambutté, E., Lotto, S., Zoccola, D., Allemand, D. and Tambutté, S.: Imaging intracellular pH in a reef coral and symbiotic anemone., Proc. Natl. Acad. Sci. U. S. A., 106(39), 16574–9, doi:10.1073/pnas.0902894106, 2009.

Venn, A. A., Tambutté, E., Holcomb, M., Laurent, J., Allemand, D. and Tambutté, S.: Impact of seawater acidification on pH at the tissue-skeleton interface and calcification in reef corals., Proc. Natl. Acad. Sci. U. S. A., 110(5), 1634–9, doi:10.1073/pnas.1216153110, 2013.

Wall, M., Fietzke, J., Schmidt, G. M., Fink, A., Hofmann, L. C., de Beer, D. and Fabricius, K. E.: Internal pH regulation facilitates in situ long-term acclimation of massive corals to end-of-century carbon dioxide conditions, Sci. Rep., 6, 30688 [online] Available from: http://dx.doi.org/10.1038/srep30688, 2016.

Wang, B.-S., You, C.-F., Huang, K.-F., Wu, S.-F., Aggarwal, S. K., Chung, C.-H. and Lin, P.-Y.: Direct separation of boron from Na-and Ca-rich matrices by sublimation for stable isotope measurement by MC-ICP-MS, Talanta, 82(4), 1378–1384, 2010.

Wei, G., McCulloch, M. T., Mortimer, G., Deng, W. and Xie, L.: Evidence for ocean acidification in the Great Barrier Reef of Australia, Geochim. Cosmochim. Acta, 73(8), 2332–2346, doi:10.1016/j.gca.2009.02.009, 2009.

Weiner, S., Traub, W. and Parker, S. B.: Macromolecules in Mollusc Shells and Their Functions in Biomineralization [and Discussion], Philos. Trans. R. Soc. B Biol. Sci., 304(1121), 425–434, doi:10.1098/rstb.1984.0036, 1984.

Wheeler, A.: Mechanisms of molluscan shell formation., in Calcification in biolgical systems, edited by E. Bonucci, pp. 179–216, CRC Press., 1992.

Wilbur, K. and Saleuddin, A.: Shell formation, in The Mollusca, edited by K. Wilbur and A. Saleuddin, pp. 235–287, Academic., 1983.

Xiao, J., Jin, Z. D., Xiao, Y. K. and He, M. Y.: Controlling factors of the δ11B-pH proxy and its research direction, Environ. Earth Sci., 71(4), 1641–1650, doi:10.1007/s12665-013-2568-8, 2014.

Yu, J., Foster, G. L., Elderfield, H., Broecker, W. S. and Clark, E.: An evaluation of benthic foraminiferal B/Ca and δ11B for deep ocean carbonate ion and pH reconstructions, Earth Planet. Sci. Lett., 293(1–2), 114–120, doi:10.1016/j.epsl.2010.02.029,

2010.

Yu, J., Thornalley, D. J. R., Rae, J. W. B. and McCave, N. I.: Calibration and application of B/Ca, Cd/Ca, and δ11B in Neogloboquadrina pachyderma (sinistral) to constrain CO2 uptake in the subpolar North Atlantic during the last deglaciation, Paleoceanography, 28(2), 237–252, doi:10.1002/palo.20024, 2013.

Zeebe, R. E.: Stable boron isotope fractionation between dissolved B(OH)3 and B(OH)4-, Geochim. Cosmochim. Acta, 69(11), 2753–2766, doi:10.1016/j.gca.2004.12.011, 2005.

Zeebe, R. E. and Sanyal, A.: Comparison of two potential strategies of planktonic foraminifera for house building: Mg2+ or H+ removal?, Geochim. Cosmochim. Acta, 66(7), 1159–1169, doi:10.1016/S0016-7037(01)00852-3, 2002.

Tables

Table 1. Protocol used to evaluate the column chemistry method of boron extraction. Three volumes of resin (60, 250 and 500 μL) were evaluated.

Step	mg resin	15	62.5	125
1	Resin (uL)	60	250	500
2	MQ H2O at pH 7 (mL)	5	5	5
3	0.5 N HNO3 (mL)	2.5	2.5	5
4	MQ H2O at pH 7 (mL) x3	2.5	2.5	5
5	Check pH			
6	Sample Load (ng)	536	536	536
7	MQ H2O at pH 7 (mL) x3	1	1	2
10	Check pH			
11	0.05N HNO3 (mL)	0.5	0.5	0.5
22	MQ H2O at pH 7 (mL)	2	2	2

Table 2. Mass spectrometer operating conditions.

	d-DIHEN	**Ammonia Addition**
Injection system	Demountable Direct Injection High-efficiency Nebulizer	PFA teflon spray chamber with ESI PFA teflon 50 μL min^{-1} nebuliser
Sample Gas Flow Rate	0.3 L min^{-}	1.1 L min^{-1}
Running Concentrations	B = 50 ppb	B = 30 – 50 ppb (evaluated 30, 65, 130 ppb)
Sensitivity	35 V ppm^{-1}, total B	20 V ppm^{-1}, total B
Blank Level	< 0.5 % of ^{11}B signal after 30s in 2 % HNO_3, 0.1 % after 120s	< 5 % of ^{11}B signal after 30s in 0.05% HNO_3, 3% after 120s
Resolution	Low	Low
Forward Power	1200 W	1200 W
Accelerating Voltage	10 kV	10 kV
Plasma Mode	Wet Plasma	Wet Plasma
Cool Gas Flow Rate	16 L min^{-1}	16 L min^{-1}
Auxiliary Gas Flow Rate	0.9 L min^{-1}	0.9 L min^{-1}
Sampler Cone	Standard Ni cone	Standard Ni cone
Skimmer Cone	X Ni cone	X Ni cone
Interferences	$^{40}Ar^{++++}$ $^{20}Ne^{++}$ resolved	$^{40}Ar^{++++}$ $^{20}Ne^{++}$ resolved
Accuracy	0.2 ‰, 2sd, n = 6	0.2 ‰, 2sd, n = 6
Acquisition	30 x 4s	30 x 4s
Baselines	Counting times of 20 s	Counting times of 20 s

Table 3. Boron isotope composition ($\delta^{11}B$; ‰) of all species evaluated, including international carbonate standards JC_P-1 (*Porites* sp.) and JCt-1 (Hard clam). Data are presented as average of *n* analyses and the precision is reported as 2 standard deviations (2SD). The cleaning protocol (Oxidised – 'Ox'/Uncleaned – 'U'), separation method ('column'/'batch'), and injection method ('NH_3'/'d-DIHEN') are presented for comparison.

Sample type	Name	$\delta^{11}B$	(2SD)	*n*	Cleaning	Separation	Injection
Hard clam	JCt-1	17.50	0.60	12	Ox	batch	d-DIHEN
Hard clam	JCt-1	16.90	0.30	6	Ox	batch	NH_3
Hard clam	JCt-1	16.34	0.64	2	Ox	column	NH_3
Hard clam	JCt-1	16.24	0.42	2	U	batch	NH_3
Porites coral	JCp-1	24.52	0.34	6	Ox	column	NH_3
Porites coral	JCp-1	24.30	0.16	10	Ox	batch	d-DIHEN
Porites coral	JCp-1	24.65	0.60	6	Ox	batch	NH_3
Porites coral	JCp-1	24.44	0.56	6	U	column	NH_3
Porites coral	JCp-1	24.41	0.30	6	U	batch	NH_3
Porites coral	JCp-1	24.36	0.51	2	Ox	column	NH_3
Porites coral	JCp-1	24.24	0.38	2	Ox	batch	NH_3
Porites coral	NEP-1	26.56	0.34	2	U	batch	NH_3
Porites coral	NEP-1	25.51	0.38	2	Ox	column	NH_3
Porites coral	NEP-1	25.34	0.78	2	Ox	batch	NH_3
Porites coral	NEP-1	25.52	0.46	2	U	column	NH_3
Porites coral	NEP-1	25.92	0.12	2	U	batch	NH_3
Porites coral	NEP-1	25.96	0.30	2	Ox	batch	NH_3
Temperate coral	OCU-9	24.04	na	1	Ox	batch	NH_3
Temperate coral	OCU-10	23.98	na	1	Ox	batch	NH_3
Temperate coral	OCU-11	24.34	na	1	Ox	batch	NH_3
Coralline alga	JR-19	39.94	0.12	2	Ox	batch	NH_3
Coralline alga	JR-20	32.65	0.46	2	Ox	batch	NH_3
Coralline alga	JR-20	32.68	0.22	2	Ox	column	NH_3
Coralline alga	JR-21	35.07	na	1	Ox	batch	NH_3
Tropical urchin	JR-56	19.00	0.36	2	Ox	batch	NH_3
Tropical urchin	JR-57	18.64	0.11	2	Ox	batch	NH_3
Tropical urchin	JR-58	18.49	0.09	2	Ox	batch	NH_3
Temperate urchin	JR-64	14.96	0.10	2	Ox	column	NH_3
Temperate urchin	JR-64	17.60	0.80	2	Ox	batch	d-DIHEN
Temperate urchin	JR-65	17.11	1.10	2	Ox	batch	NH_3
Temperate urchin	JR-66	15.43	0.11	2	Ox	batch	NH_3
Serpulid worm tube	JR-1	19.44	na	1	Ox	batch	NH_3
Serpulid worm tube	JR-2	19.13	na	1	Ox	batch	NH_3
Serpulid worm tube	JR-3	19.21	na	1	Ox	batch	NH_3
American oyster	JR125	16.18	0.16	2	Ox	column	NH_3
American oyster	JR125	15.90	0.60	2	Ox	batch	d-DIHEN
American oyster	JR125	16.00	0.32	2	U	batch	NH_3

Table 4. Summary of the average and standard deviation (SD) of $\delta^{11}B$ for each species (‰), calculated pH of calcifying fluid (pH_{CF}), pH of seawater (pH_{SW}) during the experimental conditions, difference between pH_{CF} and pH_{SW} (ΔpH), calcification response to ocean acidification experiments ('OA Response'; Ries et a;., 2009), and shell/skeletal mineralogy ('HMC' = high-Mg calcite;'LMC' = low-Mg calcite;Ries et al., 2009). In most cases 3 biological replicates of each species were analyzed. 'NA' = not available, only one biological replicate analysed. **Note:** SD is calculated from measurements of different individuals of the same species and this reflect interspecimen variability. Variability arising from intra-specimen variation (reflecting variability within a single specimen) and analytical error is provided in Table 3.

Sample Type	Scientific Name	$\delta^{11}B$ (SD)	pH_{CF}	pH_{SW}	ΔpH	OA Response	Mineralogy
Coralline alga	*Neogoniolithion* sp.	**35.89** (3.71)	9.4	8.1	1.3	Parabolic	HMC
Temperate coral	*Oculina arbuscula*	**24.12** (0.19)	8.5	8.1	0.4	Threshold	Aragonite
Tropical urchin	*Eucidaris tribuloides*	**18.71** (0.26)	8.1	8.0	0.1	Threshold	HMC
Serpulid worm	*Hydroides crucigera*	**19.26** (0.16)	8.2	8.1	0.1	Negative	Aragonite+HMC
Temperate urchin	*Arbacia punctulata*	**16.28** (0.86)	7.9	8.0	-0.1	Parabolic	HMC
American oyster	*Crassostrea virginica*	**16.03** (NA)	7.9	8.2	-0.3	Negative	LMC

Table 5. Previously published $\delta^{11}B$ analyses of biogenic marine carbonates and seawater samples

Sample	Mineralogy	$\delta^{11}B$ range (‰)	Reference
Modern Coral	Aragonite	26.7-31.9	(Vengosh et al., 1991)
Modern Coral	Aragonite	23.0-24.7	(Hemming and Hanson, 1992)
Modern Coral	Aragonite	23.5-27.0	(Gaillardet and Allègre, 1995)
Modern Coral	Aragonite	23.9-26.2	(Hemming et al., 1998)
Modern Coral	Aragonite	25.2	(Allison and Finch, 2010)
Modern Coral	Aragonite	23.56-27.88	(Anagnostou et al., 2012)
Modern Coral	Aragonite	21.5-28.0	(Dishon et al., 2015)
Modern Coral	Aragonite	21.76-23.19	(Dissard et al., 2012)
Deep Sea Coral	Calcitic	13.7-17.3	(Farmer et al., 2015)
Modern Coral	Aragonite	18.52-23.96	(Holcomb et al., 2014)
Modern Coral	Aragonite	21.1-24.9	(Hönisch et al., 2004)
Modern Coral	Aragonite	23.2-28.7	(McCulloch et al., 2012)
Deep Sea Coral	Calcitic	15.5	(McCulloch et al., 2012)
Modern Coral	Aragonite	22.5-24.0	(Reynaud et al., 2004)
Modern Coral	Aragonite	31.1-35.7	(Rollion-Bard et al., 2011a)
Modern Coral	Aragonite	18.6-30.6	(Rollion-Bard et al., 2011b)
Modern Coral	Aragonite	21-24.5	(Schoepf et al., 2014)
Modern Coral	Aragonite	23.6-25.2	(D'Olivo et al., 2015)
Ancient Coral	Aragonite	23.6-27.1	(Douville et al., 2010)
Ancient Coral	Aragonite	24.5-27.1	(Kubota et al., 2014)
Ancient Coral	Aragonite	22.5-25.5	(Liu et al., 2009)
Modern Coral	Aragonite	21.1-25.4	(Wei et al., 2009)
Planktonic Foraminifera	Calcite	14.2-19.8	(Vengosh et al., 1991)
Planktonic Foraminifera	Calcite	22.0-23.3	(Sanyal et al., 1995)
Planktonic Foraminifera	Calcite	18.4	(Sanyal et al., 1997)
Benthic Foraminifera	Calcite	13.3, 20.3, 32.0	(Vengosh et al., 1991)
Benthic Foraminifera	Calcite	20.5, 21.4	(Sanyal et al., 1995)

Bulk Foraminifera	Calcite	10.5, 11.5, 14.8, 16.2, 17.0	(Spivak et al., 1993)
Planktonic Foraminifera	Calcite	17.1, 22.9	(Kasemann et al., 2009)
Planktonic Foraminifera	Calcite	20.6-25.4	(Ni et al., 2007)
Benthic Foraminifera	Calcite	14.5-16.8	(Rae et al., 2011)
Benthic Foraminifera	Calcite	18-30.1	(Rollion-Bard and Erez, 2010)
Benthic Foraminifera	Calcite	15.8-17.4	(Yu et al., 2010)
Planktonic Foraminifera	Calcite	16.9-17.9	(Yu et al., 2013)
Planktonic Foraminifera	Calcite	19.1-22.2	(Bartoli et al., 2011)
Planktonic Foraminifera	Calcite	16.2-19.8	(Foster, 2008)
Planktonic Foraminifera	Calcite	15.2-17.2	(Foster et al., 2012)
Benthic Foraminifera	Calcite	13.09-13.37	(Foster et al., 2012))
Planktonic Foraminifera	Calcite	18.9-21.8	(Foster and Sexton, 2014)
Planktonic Foraminifera	Calcite	20.8-23.3	(Hönisch and Hemming, 2005)
Planktonic Foraminifera	Calcite	21.7-23.4	(Hönisch et al., 2009)
Benthic Foraminifera	Calcite	18.0	(Kaczmarek et al., 2015)
Planktonic Foraminifera	Calcite	15.1-16.4, 18.9-21.4	(Martínez-Botí et al., 2015a)
Planktonic Foraminifera	Calcite	19.1-19.8, 19.4-20.8	(Martínez-Botí et al., 2015b)
Planktonic Foraminifera	Calcite	24.2-25.7	(Palmer et al., 2010)
Mixed Foraminifera	Calcite	19.4-27.7	(Palmer, 1998)
Mixed Foraminifera	Calcite	20.8-26.6	(Pearson and Palmer, 1999)
Planktonic Foraminifera	Calcite	11-13.5*, 21.6-25.5	(Pearson and Palmer, 2000)
Benthic Foraminifera	Calcite	15.2-16.2	(Rae et al., 2014)
Planktonic Foraminifera	Calcite	13.6-15.8	(Penman and Hönisch, 2014)
Echinoid	High-Mg Calcite	22.7-22.9	(Hemming and Hanson, 1992)
Goniolithon	High-Mg Calcite	22.4	(Hemming and Hanson, 1992)
Encrusting Red Algae	High-Mg Calcite	23.0	(Hemming and Hanson, 1992)
Thecidellina	Calcite	21.5-22.5	(Hemming and Hanson, 1992)
Other Carbonates	Aragonite	19.1-24.8	(Hemming and Hanson, 1992)
Seawater	Seawater	39.9-40.2	(Hemming and Hanson, 1992)
Seawater	Seawater	37.7-40.4	(Foster et al., 2010)

Figures

Fig. 1. (a) Speciation of dissolved inorganic boron ($B(OH)_3$ and $B(OH)_4^-$) as a function of seawater pH. (b) $\delta^{11}B$ of dissolved inorganic boron species as a function of seawater pH. The pKb is 8.6 at 25 °C and 35 psu (Dickon, 1990), α is 1.0272 (Klochko et al., 2006), and $\delta^{11}B_{SW}$ is 39.61 (Foster et al., 2010).

Fig. 2. Plot of literature-derived $\delta^{11}B$ for corals, foraminifera and brachiopods. The two gray lines indicate the theoretical seawater borate $\delta^{11}B$-pH curves that have been applied most frequently to interpret $\delta^{11}B$ variability in marine calcifiers. The pK_B is 8.6 at 25 °C and 32 psu (Dickson, 1990).

Fig. 3. Elution curves indicating cumulative yield of boron for different volumes of the boron-specific resin (Amberlite IRA 743) placed in an ion exchange column.

Fig. 4. Boron isotopic composition (± SD) of different marine calcifying organisms as a function of seawater pH (± SD). The six species shown in this figure were grown under controlled pCO_2 conditions of *ca.* 409 ppm. Gray lines are theoretical seawater $\delta^{11}B_{B(OH)4-}$-pH curves based on different α that have been used to describe boron isotope fractionation between borate ion and boric acid in seawater (using pK_B of 8.6152 at 25°C and 32 psu). Although α = 1.0272 (Klochko et al., 2006) is presently the most commonly used α, $\delta^{11}B_{B(OH)4-}$-pH curves calculated from other values of α are also shown for reference.

Fig. 5. Exploring the potential influence of pH and boron speciation on carbonate $\delta^{11}B$ (adapted from Rollion-Bard et al., 2011b). The solid and dashed curves represent the $\delta^{11}B$ composition that would result from the incorporation of different amounts of $B(OH)_3$ into the biogenic carbonates. The dashed vertical lines represent the calculated pH based on the assumption that 0% $B(OH)_3$ is incorporated into the temperate coral skeleton and 0%, 30% and 75% $B(OH)_3$ is incorporated into the coralline algal skeleton. Of the calcite species examined, only the corraline algae has a $\delta^{11}B$ composition that could conceivably originate at least in part from $B(OH)_3$ incorporation.

Author Contribution

RAE and JBR conceived of the project and wrote the proposals that funded the work. JBR cultured the organisms. RAE, JNS, and JBR contributed to experimental design. JNS, Y-WL, MG, EP, and RAE contributed to method development. JNS performed the measurements with assistance from EP. JNS conducted the data analysis. Interpretation was led by JNS and RAE with input from JBR and Y-WL. JNS drafted the paper, which was edited by all authors.

Acknowledgements

This work was supported by the "Laboratoire d'Excellence" LabexMER (ANR-10-LABX-19) and co-funded by a grant from the French government under the program "Investissements d'Avenir", and by a grant from the Regional Council of Brittany (SAD programme). RAE and JBR also acknowledge support from National Science Foundation grants OCE-1437166 and OCE-1437371. We thank J.-P. D'Olivo and the members of the UWA lab for supplying us with an aliquot of the NEP standard.

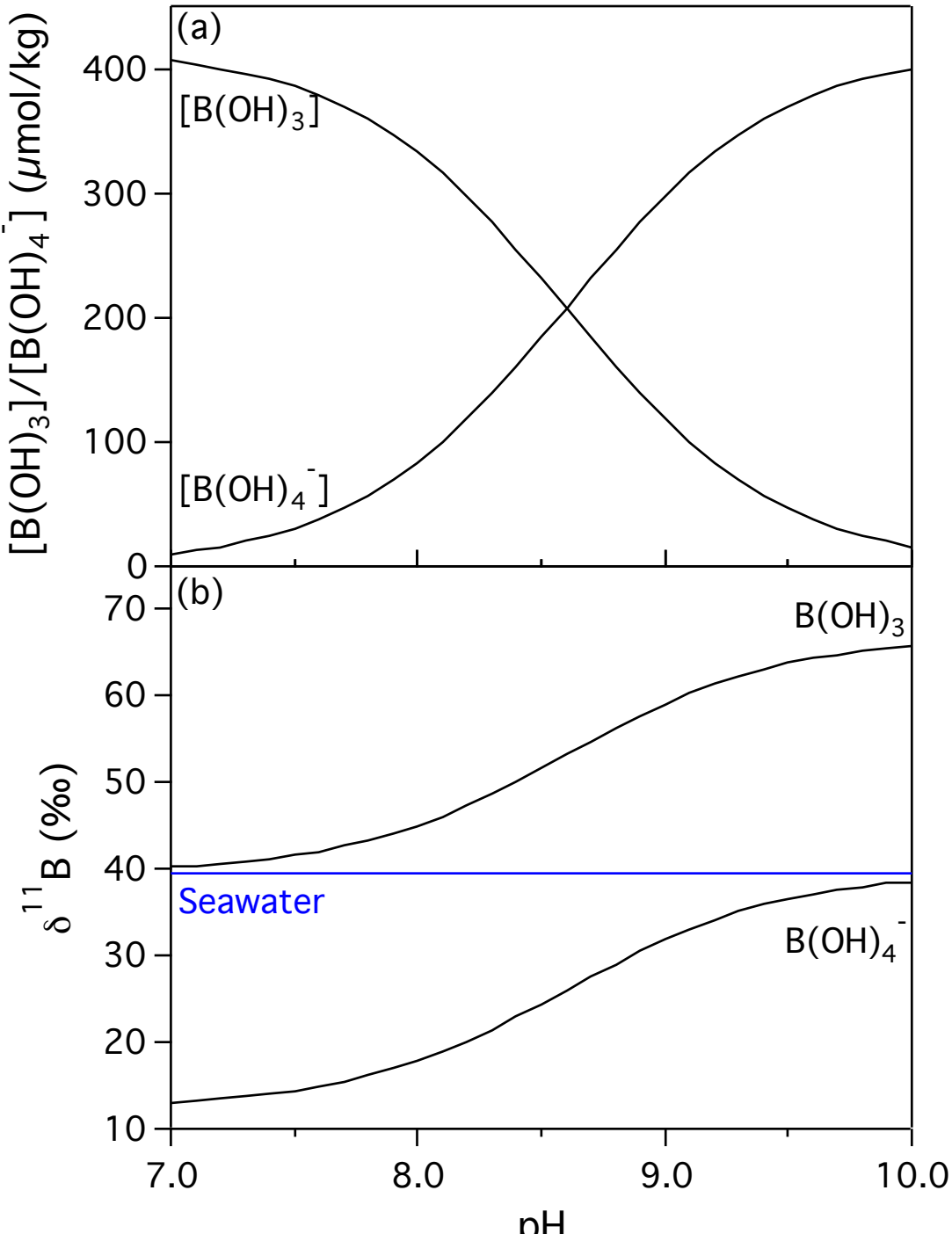
(a)
[B(OH)3]
[B(OH)4-]
[B(OH)3]/[B(OH)4-] (μmol/kg)
0
100
200
300
400
(b)
B(OH)3
Seawater
B(OH)4-
δ11B (‰)
10
20
30
40
50
60
70
7.0
8.0
9.0
10.0
pH

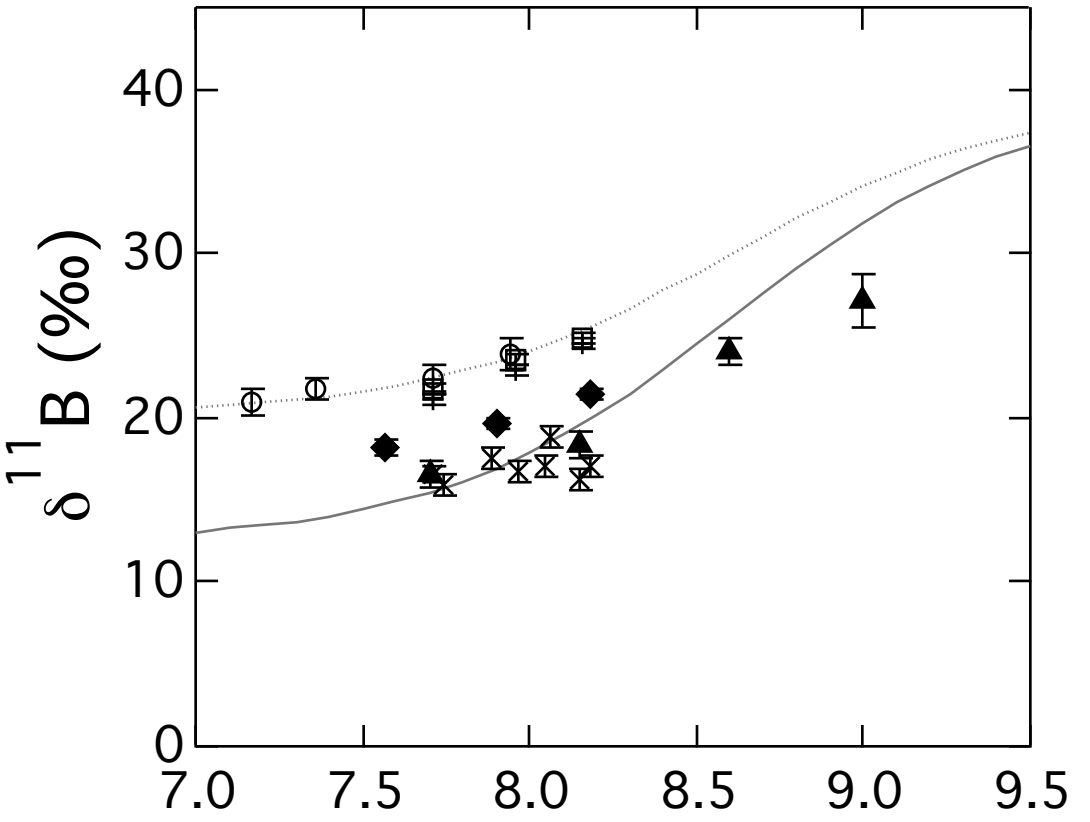

Seawater borate
α = 1.0194 (Kakihana *et al.*, 1977)

Seawater borate
α = 1.0272 (Klochko *et al.*, 2006)

\+ *Acropora nobilis* (Hönisch *et al.*, 2004)

□ *Porites cylindrica* (Hönisch *et al.* 2004)

○ *Stylophora pistillata* (Holcomb *et al.* 2014)

▲ *Orbulina universa* (Sanyal *et al.*, 1996)

◆ *Globigerinoides ruber* (Henehan *et al.*, 2013)

× Brachiopod (Penman *et al.*, 2013)

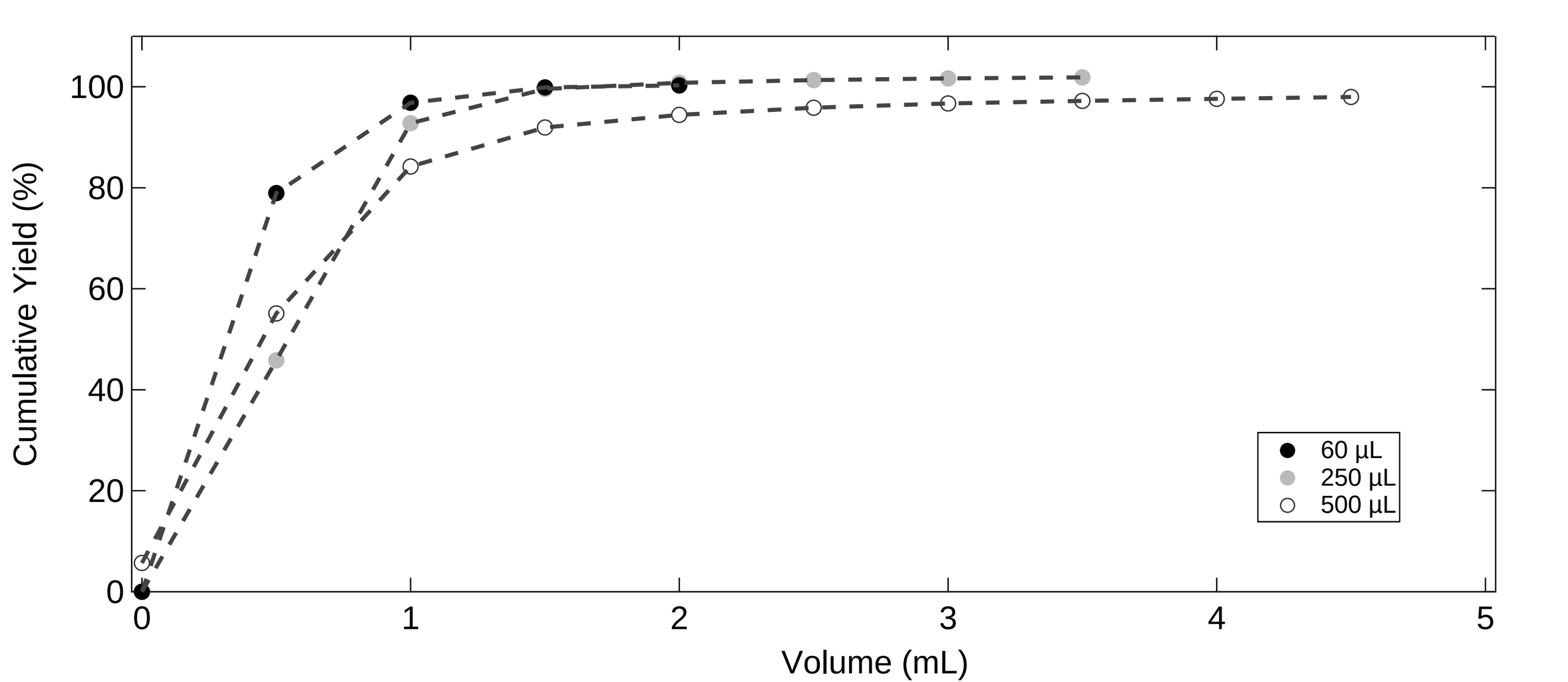
Cumulative Yield (%)
0
20
40
60
80
100
0
1
2
3
4
5
Volume (mL)
60 µL
250 µL
500 µL

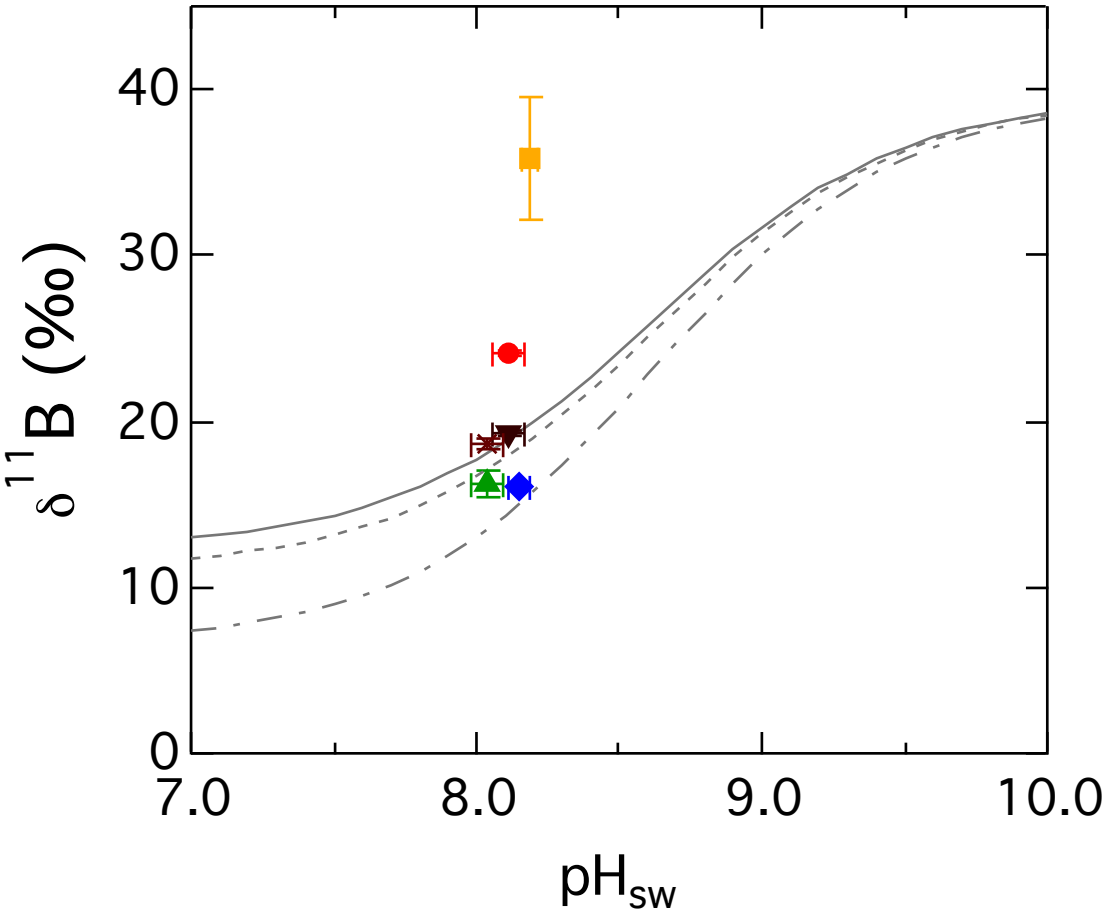

Seawater borate
α = 1.0272 (Klochko *et al.*, 2006)

Seawater borate
α = 1.0285 (Byrne *et al.*, 2006)

Seawater borate
α = 1.0330 (Palmer *et al.*, 1987)

Temperate coral
Coralline red alga
Temperate urchin
Serpulid
Tropical urchin
American oyster

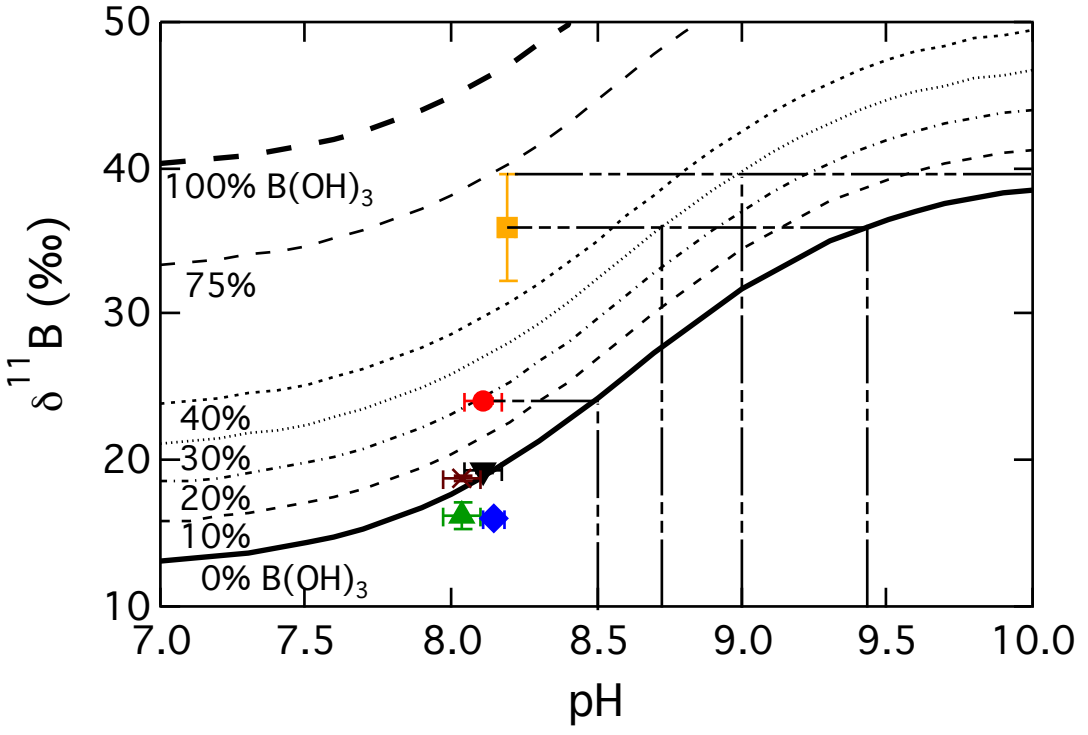
50
40
30
20
10
7.0
7.5
8.0
8.5
9.0
9.5
10.0
pH
δ 11B (‰)
100% B(OH)3
75%
40%
30%
20%
10%
0% B(OH)3
Temperate coral
Coralline red alga
Temperate urchin
Serpulid
Tropical urchin
American oyster